Assessing the Effects of Forest Treatments and Wildfires on sediment yield in the Lake Tahoe Basin

prepared by

Dr. Mariana Dobre, Research Scientist,
Department of Soil and Water Systems, University of Idaho, Moscow, ID, mdobre@uidaho.edu;

Dr. Jonathan Long, Ecologist,
USDA-FS Pacific Southwest Research Station, Davis, CA, jonathan.w.long@usda.gov;

Dr. William Elliot, Research Scientist,
Department of Soil and Water Systems, University of Idaho, Moscow, ID, welliot@moscow.com;

Dr. Erin S. Brooks, Associate Professor,
Department of Soil and Water Systems, University of Idaho, Moscow, ID, ebrooks@uidaho.edu;

Contents

I. SUMMARY

Past forest fuel management activities in the Lake Tahoe Basin have focused on the wildland/urban interface (WUI) to reduce the risk of wildfire to homes and other structures. However, given the increase in wildfire activity within the recent years, land managers within the basin are considering increasing forest treatments to more remote forested areas and on steeper slopes (30−50%), activities that have the potential to also increase soil erosion. This is a great concern in the basin since Lake Tahoe is renowned for its clear waters and eroded sediment can decrease water quality.

To address some of the managers' concerns related to increase soil erosion from forest treatments, we conducted a modeling study to simulate surface runoff and soil erosion from various management conditions followed by a series of data analyses based on the model hillslope results. We first applied the Water Erosion Prediction Project (WEPP) to all watersheds within the Lake Tahoe Basin for eleven management conditions, including current conditions, thinning, prescribed fire, and wildfire, and then performed a series of data summaries and statistical analyses to better understand the relationship between hillslope sediment yield and various environmental variables. While the main focus of the study was to specifically evaluate forest treatments on steep slopes, the large amount of data generated through this modeling exercise allowed us to expand our analyses to other environmental variables to better understand variability in sediment yield due to factors other than slope steepness.

The WEPP model was calibrated to match daily and annual values of surface runoff, sediment yield, and phosphorus, at the outlets of 17 watersheds within the basin. Overall, only minimal calibration was necessary to achieve satisfactory model performance. The model captured runoff regimes across all watersheds reasonably well, and the simulated annual trends of water yield followed the trends of observed yield. The basin-scale data summaries and statistical analyses, revealed that mechanical thinning on steeper slopes can increase soil erosion through rutting, however, current management are likely to use newer harvesting methods and equipment to minimize soil disturbance and increase ground cover. Additionally, the increases in sediment yield with thinning are not statistically significant and they need to be evaluated in terms of other ecological benefits, such as maintaining healthy ecosystems and avoiding the costs of catastrophic high severity fires.

From our analyses other variables emerged as having an influence on soil erosion, such as slope length, slope area, slope width, and precipitation. Specifically slope length appeared as an important variable in all statistical analyses, therefore managers should consider thinning activities that either include buffers or add natural breaks along the slopes (i.e. thin only portions of a slope). Since the conclusions in this study are based on modeling results and not on soil erosion from field data, these results should be used in combination with other tools and knowledge to make informed future management decisions in the Lake Tahoe Basin.

II. INTRODUCTION

Wildfire activity has been increasing since the mid-1980s in the western U.S. (Westerling et al., 2006) and multiple recent studies suggest that it will continue to increase in the next decades (Yue et al., 2014, Williams et al., 2019, Higuera and Abatzoglou 2021). Within the state of California there was a fivefold increase in annual burned area between 1972−2018 (Williams et al., 2019), with year 2020 experiencing five of the six largest wildfires in state history (Higuera and Abatzoglou 2021). The increase in wildfire activity is mainly attributed to anthropogenic climate changes, specifically to shifts in land use and land use practices, among others (Abatzoglou et al., 2020, Bowman et al., 2020, Coop et al., 2020). In the largely forested areas of the Sierra Nevada mountains, the burned areas are projected to increase by 50% by midcentury. Similarly, Williams et al. (2019) projected an eightfold increase in annual summer forest-fire extent in forested North Coast and Sierra Nevada regions. These statistics are concerning for land and water managers responsible for protecting natural resources.

Forest treatments, especially mechanical thinning and prescribed fires have been proposed as effective measures to reduce wildfire risks (Schwilk et al., 2009, Agee and Skinner, 2005) but also to improve forest resistance to drought and to restore forest structure to historic conditions (Low, 2021). Despite these recommendations, some forest treatments, such as prescribed fires, are still not widely implemented, which is attributed to various factors including favorable weather for burning, air quality constrains, and negative social perception (Kolden 2019).

Fuel reduction treatments using mechanical equipment have commonly been limited to slopes less than 40% on national forest lands in the Sierra Nevada (North et al., 2015). In the Lake Tahoe Basin, regulatory agencies had limited treatments on slopes greater than 30% based on the Bailey Land Capability System developed in the 1970s (Long, 2009), limitations that are mainly driven by water quality and clarity standards (Safford et al., 2009). However, agencies in the Lake Tahoe Basin and other parts of the Sierra Nevada are now interested in the potential benefits and risks of conducting fuel reduction and forest restoration treatments, specifically ground-based thinning using heavy equipment, on slopes greater than 30% to reduce the potential risk of wildfires.

More recently, land managers and scientists have been warned that treatments on steep slopes are important to reduce the potential impacts of severe wildfires (Long, 2009). For example, following the Angora Fire (2007), Safford et al., 2009 examined the effects of previous fuel treatments on fire severity and reported that an area of steeper slopes had been treated only with hand-thinning and consequently experienced more severe fire; the study also noted that forest thinning on steep slopes needs to be more extensive to achieve a similar fire hazard reduction as on gentle slopes.

Some research has cautioned that slope steepness is a risk factor for soil erosion, but many studies have not found it to be a significant driver of erosion rates. For example, one study (Fox and Bryan, 2000)

noted a general slope-erosion relationship, finding that "for a constant runoff rate, soil loss increased roughly with the square root of slope gradient." However, another study found that steep slopes develop geomorphic features that moderate erosional energy (Giménez and Govers, 2001). A study in New Mexico (Cram et al., 2007) found that steep slopes (26% to 43%) in a mixed-conifer forest in central New Mexico were potentially susceptible to rutting from tires on equipment, and they noted that exposed bare soil was a key indicator. When litter was disturbed but not displaced (characterized as only light to moderate disturbance), runoff and sedimentation on steep slopes did not exceed non-disturbed sites. The authors concluded that advanced equipment such as forwarding beds can avoid erosion from surface disturbance.

The general concern that steep slopes are vulnerable to erosion is often linked to practices sometimes associated with mechanical harvest including clearing and road or trail construction that reduce root strength and increase water runoff (Sidle et al., 2006). Such pronounced effects are unlikely to result from fuel reduction thinning that adheres to best management practices (BMPs), such as limiting the extent and connectivity of disturbed areas (e.g. designated location for landing and spacing of skid trails and burn piles).

Forest treatments, slope steepness, and soil erosion in the basin

Land managers in the Lake Tahoe Basin are focused on harvest using ground-based machines, although cable-yarding and loaders have been considered as alternative harvest technologies for steep slopes (Han and Han, 2020); such treatments pose different risks in terms of erosion, with little risk where logs can be fully suspended.

A field study of erosion risk from thinning and prescribed burning was conducted in the Lake Tahoe Basin (Harrison et al., 2016); that study included four sites with slopes exceeding 30% (Table 1):

Table 1: Sites with slope over 30% in a field study of erosion in the Lake Tahoe Basin.

Site	Avg. slope (%)	Soil type	Parent material	Hydraulic conductivity (cm s^{-1})	Bulk density (field) (g cm^{-3})
Incline 1	38	JO-TA	Volcanic	0.001	0.89
Incline 2	38	JO-TA	Volcanic	0.001	1.16
Slaughterhouse 1	35	CS-CG	Granitic	0.001	1.11
Slaughterhouse 2	34	CS-CG	Granitic	0.006	1.23

JO-TA = Jorge-Tahoma; CS-CG = Cassenai-Cagwin

In their results for mastication and prescribed burning, slope was not a significant predictor of erosion. No sediment yield was observed for plots with up to 60% of the surface area burned, despite steep slopes. The authors observed that several practices commonly used in the basin likely limited erosion effects, including dry season operations, limited passes with equipment, application of slash in trails, and use of low ground-pressure vehicles, as has been reported from other areas (Zamora-Cristales et al., 2014). They also noted that steeper slopes were unlikely to be treated with mastication and less

likely to be treated with prescribed fire due to implementation challenges. However, they noted that their results "should not be extrapolated to steeper sites".

A recent follow-up to a pile burning study in the basin noted that pile burning generally did not pose erosion hazards. However, the researchers found that one site, which had not reestablished vegetative cover after several years, was located on a steep slope (Busse et al., 2018). Despite that issue, the authors noted that the eroded sediments did not move far down slope.

A review of fuel treatment effects on soils (Verburg et al., 2009) mentioned some earlier field studies in the basin and cited a rainfall simulation experiment on granitic soils (Cagwin series). The study found that interrill erosion increased significantly as slope class increased from 15−30% to greater than 30%, but slope had no significant effect on infiltration and runoff (Guerrant et al., 1991). They also noted that soil type appeared to have relative low erosion risk. A follow-up study (Naslas et al., 1994) conducted on three slope classes (<15%, 15−30%, >30%), found that erodibility was more dependent on soil type, plot condition and duration of a rainfall event rather than steepness. Those studies suggested that more simplistic classification systems, like the Bailey system, were insufficient to evaluate erosion potential.

Studies from Wildfire Settings

Several studies in wildfire contexts have not found slope to be a main contributor to erosion, especially where the slope exceeds 10−20%. In a study in Colorado, Benavides-Solorio and MacDonald (2005) measured the rates of sediment yield at 48 hillslope-scale plots from three prescribed fires and three wildfires. The authors then quantified the effects of various environmental variables (including slope) on sediment yield and developed empirical models to predict post-fire sediment. Approximately 77% of the model variability in sediment production rates was explained by percent bare soil, rainfall erosivity, fire severity, soil water repellency, and soil texture. Surprisingly, slope was not selected by any of the predicted models, which the authors attributed to the lower variability in slopes (25−45%).

Similar results were found in a separate study, also in Colorado, where slope had limiting effects on sediment yield (Pietraszek, 2006). The authors also attributed these results to the lower variability in slope steepness (20−40%).

Slope steepness was also not important in a study in Montana where the authors found that 75% of the variance in first-year post-fire hillslope erosion rates was explained by the 10-minute rainfall intensity (I_{10}). Other site characteristics, such as ground cover, water repellent soil conditions, and slope steepness were obscured when I_{10} was greater than 70 mm/h (Spigel and Robichaud, 2007).

Effects of ground cover on soil erosion

The most critical influence of management on soil erosion is through its effect vegetative residue (live plants, wood, or litter) covering the soil. Rock fragments can also provide soil protection from raindrop splash, aggregate disintegration, and detachment by overland flow. The role of ground cover on limiting soil erosion applies throughout forested landscapes. Consequently, when using any model to project erosion in forested landscapes, the effects of natural disturbances like wildfire as well as management activities such as thinning, prescribed fire, trails and roads on ground cover are critical.

Forest fuel reduction efforts attempt to reduce surface fuels while maintaining sufficient ground cover to inhibit erosion. In practices observed in the Lake Tahoe Basin, residual ground covers are likely to be effective. Research by Harrison et al. (2016) confirmed that even relatively low (25%) levels of ground cover, in the form of masticated fuels or duff, could effectively inhibit erosion, and that maintaining patchy ground cover could be more beneficial than maintaining continuous ground cover.

Concerns with parameters other than ground cover

Studies of soil quality and forest treatment effects have often examined soil compaction, and that indicator has been a focus of soil monitoring in the basin (Norman et al., 2008). Compaction by heavy equipment can have negative impacts on vegetation, particularly seedlings (Mariotti et al., 2020). However, such concerns may be less significant for fuel reduction contexts in the Lake Tahoe Basin, where treatments commonly occur on coarsely-textured granitic soils and are expected to reduce small trees. While compaction is important for hydrology (change in infiltration leads to increased overland flow and potential for erosion), the amount of cover is a more direct control on erosion rates (Prats et al., 2019). One concern is that wheeled or tracked vehicles might be more subject to slippage on steep slopes, which could lead to gouging of soils, but experienced operators and oversight may limit or mitigate such potential.

III. METHODS

The WEPP model

The Water Erosion Prediction Project (WEPP) model is a physically-based, continuous-simulation, distributed-parameter model (Flanagan and Nearing, 1995). The WEPP technology is based on the fundamentals of hydrologic and erosion science (Nearing et al., 1990) and has been initially developed and successfully applied to predict soil erosion from small agricultural catchments (Flanagan and Nearing, 1995, Flanagan et. al., 2007). However, in the recent years the model has been improved to predict sediment delivery from larger forested watersheds. Major recent improvements include the incorporation of the Muskingum-Cunge channel routing algorithms (Wang et al, 2014) and of a simple linear reservoir algorithm (Srivastava et al., 2013, Srivastava et al., 2017, and Srivastava et al., 2018, Brooks et al., 2016), which now allows users to apply the model to larger watersheds characterized by baseflow.

The WEPPCloud online GIS interface

WEPPcloud (https://wepp.cloud) is an online interface for the WEPP model that allows users to run hydrologic simulations and view model results without downloading any data or software on their computers. To run predictions of runoff and erosion, users only need a computer connected to the internet. All input, output, and model runs are stored online and can be accessed by the user at a later time or shared with other collaborators. The Lake Tahoe interface (https://wepp.cloud/weppcloud/lt/) is site-specific and all input data, especially the management files, were specifically created for this project based on data from literature and from previous field measurements.

Study sites and watershed delineation

For this study, we selected all watersheds around the Lake Tahoe Basin (Fig. 1), with a few exceptions. We excluded ski runs because treatments at such sites are likely to differ from the general forest and would require more customization. Similarly, urban areas and small "frontal" watersheds that are concentrated in the Wildland-Urban Interface (WUI) were not specifically modeled because WEPP was designed as a wildland model. Urban areas with impervious surfaces require more complex calibration and customization of input parameters. The Lower Truckee watershed in the NW side of the lake flows out of the basin. Therefore, this area was excluded from the analyses.

The watersheds were delineated based on a USGS National Elevation Dataset (NED) at 30-m resolution using the TOPAZ (Garbrecht and Martz, 1999) model. Two parameters are needed to delineate watersheds: a Critical Source Area (CSA—the threshold area at which the channel begins) and a Minimum Source Channel Length (MSCL—the minimum length of a channel). Higher MSCL and CSA values will delineate watersheds with less number of hillslopes but longer lengths, while smaller values will delineate more number of hillslopes but shorter lengths. In the current simulations we used MSCL = 60 and CSA = 5.

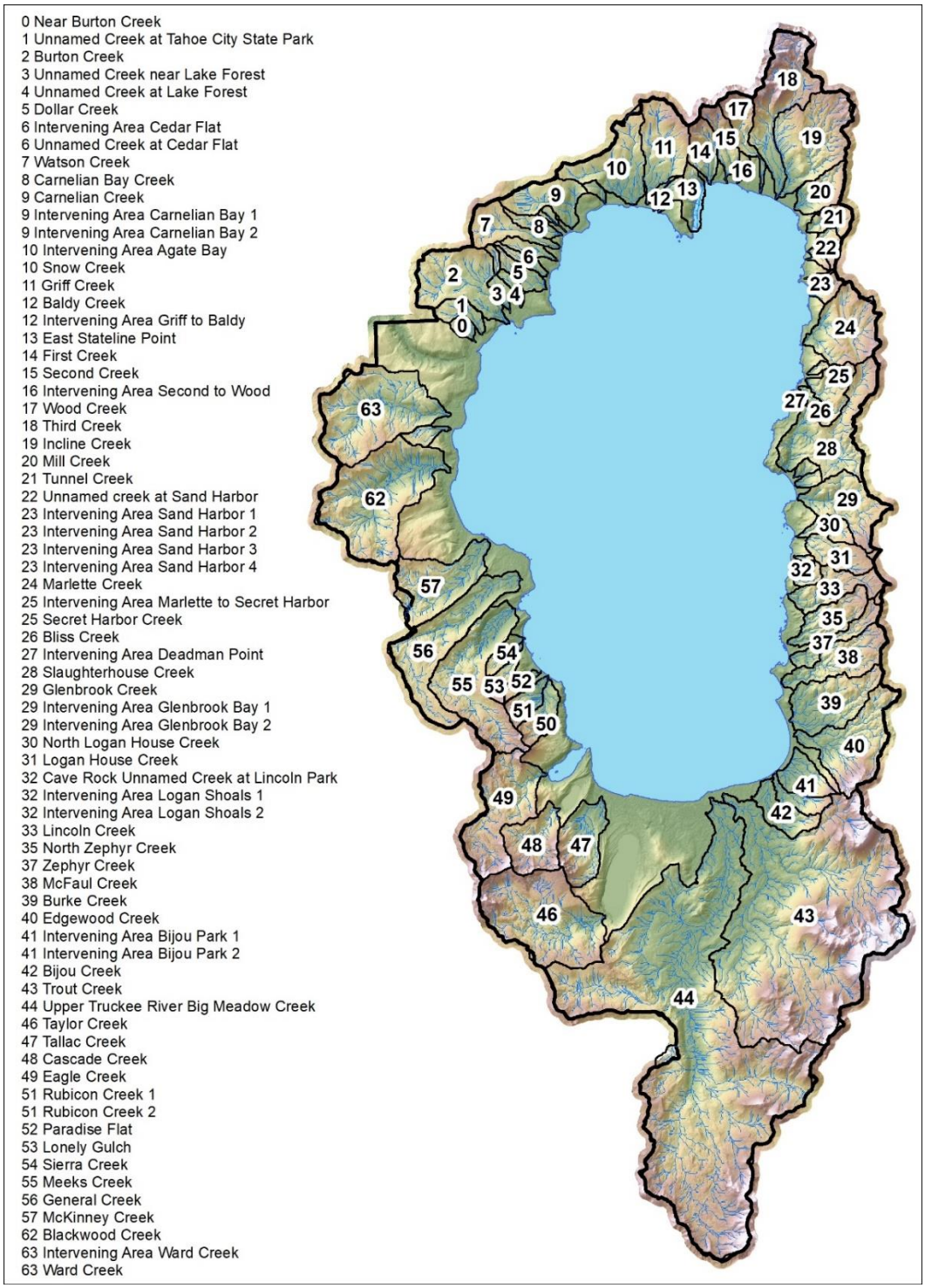

Fig. 1. Watershed boundaries and names of the simulated watersheds.

Model setup and input data

Soils and Landcover/Managements

The soil and management files are created based on default values in WEPP or are extracted from national databases. The WEPP soil input files require: *rill* and *interrill erodibility*, *critical shear*, *effective hydraulic conductivity*, *soil depth*, *%sand*, *%silt*, *%clay*, *%rock*, *%organic matter*, *CEC*, *bulk density*, *hydraulic conductivity*, *wilting point*, and *field capacity* for each soil layer. We automatically extracted all these parameters from the NRCS SSURGO database and created a soil file for each hillslope in each watershed. Similarly, we identified a landcover type based on the 2016 NCDL Landcover map (e.g. deciduous forest, evergreen forest, shrubland, etc.) and then created a Tahoe-specific WEPP management file similar to Brooks et al., 2016, and assigned it to each hillslope. Although WEPP requires several vegetative parameters, the most sensitive ones are %canopy cover, %rill and %interrill ground covers, and Leaf Area Index (LAI). These input files were the basis for the "Current Conditions" scenario.

Weather data

In the Lake Tahoe model runs we used the historic gridded Daymet at 1 km spatial resolution (Thornton et al. 2016) database to acquire daily precipitation, maximum and minimum temperature at each hillslope within the modeled watersheds between 1990–2019. The rest of the weather parameters (storm duration, time to peak intensity, peak intensity, solar radiation, average wind speed and duration, and dew point temperature) were stochastically generated based on the nearby Tahoe, CA station, using the CLIGEN weather generator (Nicks and Lane 1989, Srivastava et al. 2019).

For the future climate scenario, we used the A2 climate scenario (Coats et al., 2013) for the daily precipitation, maximum and minimum temperature and CLIGEN for the remaining parameters. An important observation is that the CLIGEN model uses current weather stations to generate local storm durations and intensities and, therefore, might not be comparable to future storm characteristics. Future model simulations are between 2018–2048. The weather files were built to match the streamflow and water quality data available at the outlet of the modeled watersheds (Table 2).

Model calibration and performance assessment

Model accuracy assessment was performed on 17 watersheds in the basin with long-term observed USGS data (Fig. 2; Table 2). To calibrate the model, we ran the WEPPcloud interface with default parameters and downloaded all the model runs (including all the input and output data) with the wepppy-win-bootstrap, a freely available Python package developed to allow advanced users to download, modify, and run WEPPcloud projects locally on Windows computers (Lew, 2021). We first calibrated daily streamflow and total water yield as described below and then calibrated key parameters related to sediment and phosphorus yield. Model performance was assessed for each watershed simulation by utilizing a variety of publicly available USGS data sources: daily streamflow data measured at USGS gauging stations, flow-weighted annual loads of sediment and phosphorus processed in previous studies, and flow-weighted monthly concentrations of phosphorus. Model performance efficiency was assessed using several goodness-of-fit statistics: the Nash-Sutcliffe Efficiency (*NSE*; Nash and Sutcliffe, 1970), the Kling-Gupta efficiency (*KGE*; Gupta et al., 2009), and

percent bias (*PBias* (%); Yapo et al., 1996). These indices were calculated with the '*hydroGOF'* R package (Zambrano-Bigiarini, 2020).

Table 2. List of gauged study watersheds, simulation dates, areas, elevations, and precipitation. Full USGS station codes and names, the corresponding WEPPcloud interface model run names, and web addresses for the model runs are provided in the supplementary material (Table A1 in Appendix).

No.	Name	USGS station	Simulation date range YYYY/MM/DD		Watershed area	Min. elevation	Max. elevation	Mean Annual Precipitation
			Start	End	(ha)	(m)	(m)	(mm)
					California			
1	WC8§	10336676	1990/01/01	2014/09/30	2310	1920	2700	1406
2	WC7A§	10336675	1991/10/01	2001/09/30	2170	1967	2700	1414
3	WC3A§	10336674	1991/10/01	2011/11/01	1160	2021	2700	1496
4	BC1	10336660	1990/01/01	2014/09/30	2670	1904	2676	1476
5	GC1	10336645	1990/01/01	2014/09/30	1820	1913	2640	1271
6	UTR1§	10336610	1990/01/01	2014/09/30	13320	1899	3052	1025
7	UTR3§	103366092	1990/06/01	2012/09/30	9380	1926	3050	1117
8	UTR5§	10336580	1990/05/12	2011/10/11	3410	1981	3050	1218
9	TC4§	10336780	1990/01/01	2014/09/30	9870	1899	3306	905
10	TC2§	10336775	1990/06/01	2012/09/30	5560	1914	3259	880
11	TC3§	10336770	1990/05/22	2011/03/31	1780	2124	3259	900
					Nevada			
12	LH1	10336740	1990/01/01	2011/10/12	500	2030	2688	657
13	GL1	10336730	1990/01/01	2012/09/30	990	1903	2689	616
14	IN1§	10336700	1990/01/01	2014/09/30	1580	1904	2807	928
15	IN2§	103366995	1990/01/01	2004/09/30	1070	1942	2807	999
16	IN3§	103366993	1990/05/01	2011/03/31	690	2114	2807	1061
17	TH1	10336698	1990/01/01	2014/09/30	1470	1900	3135	1081

§ *Denotes nested watersheds.*

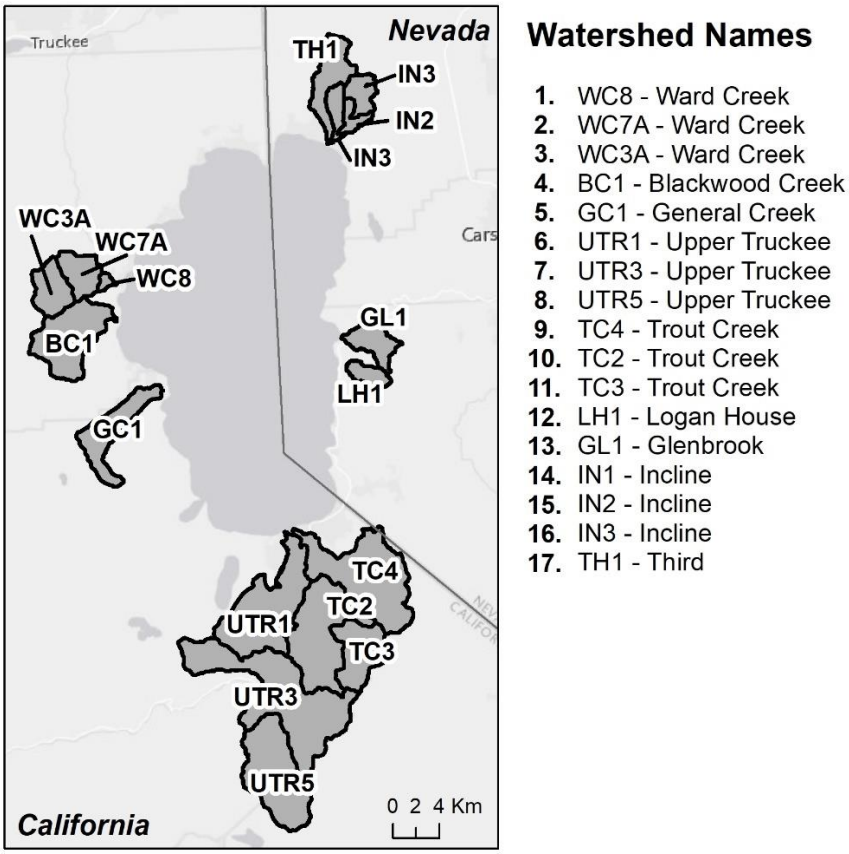

Fig. 2. Watersheds with observed data used for calibration.

Streamflow and water yield

Streamflow calibration was performed using only the linear baseflow recession coefficient (k_b). The k_b coefficient represents the fixed proportion of the total water stored in a dynamic groundwater reservoir that provides baseflow to the stream on any given day and typically varies between 0.01 d^{-1} and 0.1 d^{-1} (Beck et al., 2013; Sánchez-Murillo et al., 2014). Brooks et al. (2016) determined that the observed streamflow recessions on the western side of Lake Tahoe could be represented by a linear reservoir coefficient k_b of 0.04 d^{-1}. However, due to a complex hydrogeology of the east side of the Lake Tahoe Basin, attributed to large geologic faults and high permeability rates (Nolan and Hill, 1991), the authors proposed that additional deep seepage losses of groundwater were occurring and suggested that the rate of groundwater loss from the reservoir could be quantified by calibrating a second deep seepage reservoir coefficient (k_s) for groundwater lost from the system. For our simulations, we assigned a default k_b value of 0.04 d^{-1} to all modeled watersheds from the west-side of the basin and calibrated the k_b and k_s coefficients for the east-side watersheds similar to the Brooks et al. (2016) approach. For the streamflow model performance assessment, we used a maximum of 25 years (1990–2014) of observed daily streamflow data at the 17 watersheds identified in Table 2.

Sediment yield

The WEPP model can simulate soil erosion from hillslopes and channels, soil deposition within the hillslope and channel profile, and sediment yield at the watershed outlet. The most important calibrating parameters for simulating soil erosion are effective hydraulic conductivity, rill and interrill erodibilities, hillslope critical shear, percent ground cover, and channel bed critical shear stress (τ_c) (Nearing et al., 1990). For hillslopes, these parameters were set by default in the WEPPcloud interface based on previous field observations in forest soils of various textures (Lew et al., 2021). Similarly, for channel erosion, Srivastava et al. (2020) demonstrated good agreement between observed and model simulations in the seven watersheds in the Mica Creek Experimental Watershed in North Idaho (MCEW) by varying only the channel τ_c. The authors found a direct relationship between WEPP-calibrated τ_c and the median particle size (D_{50}) and suggested that pebble count data can be used to parametrize the channel τ_c in forested watersheds. In the Lake Tahoe watersheds, pebble count data were available at few locations, which were provided by the land managers. We calculated the D_{50} from the observed pebble count data and identified the channel bed critical shear stress-equivalent following Berenbrock and Tranmer (2008).

Observations of event-based suspended sediment concentrations (SSC) were available at the USGS gauging stations for all modeled watersheds in the Lake Tahoe Basin. Additionally, we also had available flow-weighted annual loads of SSC estimated in a previous study in the basin by Coats et al. (2016). The authors estimated and compared annual loads from several regression equations after correcting the sources of bias in the USGS water quality database.

Phosphorus yield

Simulated phosphorus yield in WEPPcloud is based on simple static phosphorus concentrations in each of the three components of the streamflow hydrograph (surface runoff, subsurface lateral flow, and baseflow), and particulate phosphorus concentration on the delivered sediment. These static concentrations were calculated based on long term observed streamflow (*USGS code: 00060—Discharge, $ft^3\ s^{-1}$*) and event-based TP concentrations (*USGS code: 00665—Phosphorus, water, unfiltered, $mg\ l^{-1}\ P$*), SRP (*USGS code: 00671—Orthophosphate, water, filtered, $mg\ l^{-1}\ P$*), SSC (*USGS code: 80154—Suspended sediment concentration, $mg\ l^{-1}$*), and streamflow (*USGS code: 00061—Discharge, instantaneous, $ft^3\ s^{-1}$*) measured at the USGS stream gauging stations and bias-corrected by Coats et al., 2016. Particulate phosphorus (PP; $mg\ L^{-1}$) is not typically measured at the USGS stream gauging stations and was calculated by subtracting SRP from TP. Since these observations were event-based, we calculated the flow-adjusted daily concentrations with the LOAD ESTimator (LOADEST; Runkel et al., 2004) model, which is a USGS model used to derive relationships between event-based streamflow and suspended sediment concentrations based on eleven pre-defined regression equations. For each watershed, we ran the LOADEST model with an automated regression model selection.

On 1 January 1997 and 31 December 2005, a few watersheds on the western side of the Lake Tahoe experienced significant rain-on-snow events that caused record peak streamflow events. For example, Blackwood Creek, USGS code 10336660, recorded 83 $m^3\ s^{-1}$ (247 mm) in 1997 and 64 $m^3\ s^{-1}$ (191 mm) in 2005 peak streamflow. Therefore, when using the entire data record generated bias model

results, we ran seasonally piecewise LOADEST models for all years except for WY 1997 and WY 2006, and then separately for years WY 1997 and WY 2006. Gao et al. (2018) found that the seasonally piecewise method performed better than the year-round method in estimating monthly nitrogen loads.

Static phosphorus concentrations needed as input to the WEPPcloud interface were further calculated from the flow-weighted concentrations for each watershed. We assumed the phosphorus concentrations in the surface runoff are typical of the streamflow SRP concentrations (mg L^{-1}) during spring snowmelt (months April and May) and that the phosphorus concentrations in the baseflow are typical of the streamflow SRP concentrations (mg L^{-1}) in the fall (September and October). For the phosphorus concentrations in lateral flow, we averaged the SRP streamflow concentrations (mg L^{-1}) of the remaining months. We calculated the particulate phosphorus concentrations adsorbed to sediments with equation 1.

$$pSediment = \left(\frac{TP - SRP}{SSC}\right) 10^6 \quad (1)$$

where $pSediment$ is the particulate phosphorus concentration (mg kg^{-1}), calculated for May, which is the month with the highest runoff and SSC. We used the phosphorus concentrations determined from the observed data as initial input to the model and further calibrated these values to match simulated values with observed annual average flow-adjusted loads of TP, SRP, and PP.

Model parameterization for management scenario testing

For this analysis, we modeled 72 watersheds identified in Fig. 1 for 11 management scenarios, or conditions. The management parameters used to simulate these conditions are provided in Table 3.

Management conditions:

1. *Undisturbed Current Conditions.*
2. *Uniform Thinning (96% Cover)*
3. *Uniform Thinning (Cable 93% Cover)*
4. *Uniform Thinning (Skidder 85% Cover)*
5. *Uniform Prescribed Fire*
6. *Uniform Low Severity Fire*
7. *Uniform Moderate Severity Fire*
8. *Uniform High Severity Fire*
9. *Simulated Wildfire – FCCS fuels – current conditions*
10. *Simulated Wildfire – future fuels from LANDIS and current climate*
11. *Simulated Wildfire – future fuels from LANDIS and future climate scenario A2*

The purpose for simulating undisturbed conditions was to establish a baseline for sediment and phosphorus that managers could use for comparing impacts of alternative management strategies to current conditions. For those watersheds that were gauged, the undisturbed conditions also provided an opportunity to more finely calibrate the model. The vegetation types for the current conditions assumed 100% ground cover in forested areas and 90% in the shrub-dominated areas.

Thinning and burning scenarios were simulated assuming the entire watershed was exposed to the same condition at once, although it is improbable that a fire would uniformly burn an entire watershed or that thinning would occur on all hillslopes at once. Thinning assumed 96, 93, and 85% ground cover in forested areas, with no treatment in other vegetation types. While the method of thinning does not necessarily affect the number of trees removed, it does affect the post-disturbance ground cover. We assumed the three thinning scenarios to be representative of hand thinning (96% post-disturbance ground cover), cable thinning (93%), and skidder thinning (85%), respectively. Of all thinning methods, hand thinning has the lowest ground cover disturbance. In Lake Tahoe, this method has been applied mainly on steep slopes, where there are concerns with soil disturbance by heavy equipment (Lake Tahoe Basin Report, 2014). Mechanical thinning is more cost-effective than hand thinning, however it is prohibited in the basin on slopes greater than 30 percent and on sensitive areas (e.g. stream environment zone). We also assumed the 96% mechanical treatment to be similar to cable-based thinning methods while 85% to be similar to skidder thinning. Most thinning treatments in the basin are already designed to minimize soil disturbance and, across the basin, average post-thinning ground cover varies between 87 and 100% (Norman et al., 2008, Pell and Gross, 2016, Christensen and Norman, 2007). Therefore, we considered the 85% post-disturbance ground cover as an extreme thinning scenario, which we used in several statistical analyses.

Prescribed fire, low, moderate, and high severity fire management conditions assumed ground covers of 85, 80, 60, and 30%, respectively, in forested areas, 75, 70, 50, and 30%, respectively, in shrub-dominated areas, and no treatment in other vegetation types. Similar to the thinning scenarios, the uniform application of a scenario tends to increase the overall sediment yield at the outlet of a watershed, but it allowed us to directly compare simulated runoff, sediment, and phosphorus for each hillslope and watershed from all management conditions.

The runs with a simulated wildfire were based on predicted Soil Burn Severity (SBS) map. These maps assign either a low, moderate or high soil burn severity to each hillslope in the basin and were created based on a machine learning technique in which we used historic SBS maps from the King, Angora, and Emerald fires with several environmental variable related to soils, topography, climate, landcover, and fuels, to predict SBS classes of low moderate, and high severity for the entire Lake Tahoe Basin. The fuel loads were based on both FCCS and LANDIS. FCCS is the "Fuel Characteristic Classification System" (Ottmar et al., 2007) and LANDIS is a vegetation growth model that can be driven by historic or future climates (Scheller et al. 2007).

Soil properties vary with soil type (e.g. granitic, volcanic) and land use (e.g. forest, shrubs, grass) and they change with changes in land management or with wildfire. To reflect a change in management, such as thinning, prescribed fire, or a wildfire, we altered key soils and management parameters based on filed validated measures (Elliot, 2004) (Table 3).

For this study we delineated 72 watersheds that drain directly into the lake, but only 17 watersheds have water quality observations for calibration. The k_b and k_s, channel τ_c, and phosphorus concentrations in surface runoff, subsurface lateral flow, baseflow, and sediment for the calibrated watershed runs were distributed to uncalibrated watersheds across the basin based on the watershed's similarities, parent material, and proximity.

All simulations were performed using Python batch processing scripts that generate WEPPcloud compatible projects and results were further compiled in tabular data files and GIS data files. In the current version of the WEPPcloud interface, users can perform similar scenario testing for only individual watersheds, however, future interface developments will allow select users to perform similar batch hydrologic modeling for multiple watersheds and scenarios at the same time.

Table 3. Key hillslope soils and management parameters used to parameterize the WEPPcloud interface by management and three soil types, for the study watersheds.

		Soils			Managements		
Soil Type	**Management Name**	**Critical Shear (Pa)**	**Interrill Erodibility (Kg s/m4)**	**Rill Erodibility (s/m)**	**Canopy Cover (fraction)**	**Interril Cover (fraction)**	**Rill Cover (fraction)**
Granitic	Old Forest	4	250000	0.00015	0.9	1	1
Granitic	Young Forest	4	400000	0.0002	0.8	1	1
Granitic	Forest Thinning 96% cover	4	400000	0.00004	0.4	0.96	0.96
Granitic	Forest Thinning 93% cover	4	400000	0.00004	0.4	0.93	0.93
Granitic	Forest Thinning 85% cover	4	400000	0.00004	0.4	0.85	0.85
Granitic	Forest Prescribed Fire	4	1000000	0.0003	0.85	0.85	0.85
Granitic	Forest Low Severity Fire	4	1000000	0.0003	0.75	0.8	0.8
Granitic	Forest Moderate Severity Fire	4	1000000	0.0003	0.4	0.5	0.5
Granitic	Forest High Severity Fire	4	1800000	0.0005	0.2	0.3	0.3
Granitic	Shrubs	4	141100	0.0000873	0.7	0.9	0.9
Granitic	Shrub Prescribed Fire	4	170100	0.000149	0.7	0.75	0.75
Granitic	Shrub Low Severity Fire	4	170100	0.000149	0.5	0.7	0.7
Granitic	Shrub Moderate Severity Fire	4	170100	0.000149	0.3	0.5	0.5
Granitic	Shrub High Severity Fire	4	948600	0.0004343	0.05	0.3	0.3
Granitic	Bare Slope	4	300000	0.005	0.05	0.2	0.2
Granitic	Sod Grass	4	196700	0.0004446	0.4	0.6	0.6
Granitic	Bunch Grass	4	196700	0.0004446	0.6	0.8	0.8
Alluvial	Old Forest	1	300000	0.0001	0.9	1	1
Alluvial	Young Forest	1	500000	0.00015	0.8	1	1
Alluvial	Forest Thinning 96% cover	1	500000	0.00003	0.4	0.96	0.96
Alluvial	Forest Thinning 93% cover	1	500000	0.00003	0.4	0.93	0.93
Alluvial	Forest Thinning 85% cover	1	500000	0.00003	0.4	0.85	0.85
Alluvial	Forest Prescribed Fire	1	1500000	0.0002	0.85	0.85	0.85
Alluvial	Forest Low Severity Fire	1	1500000	0.0002	0.75	0.8	0.8
Alluvial	Forest Moderate Severity Fire	1	1500000	0.0002	0.4	0.5	0.5
Alluvial	Forest High Severity Fire	1	2000000	0.0004	0.2	0.3	0.3
Alluvial	Shrubs	1	141100	0.0000873	0.7	0.9	0.9
Alluvial	Shrub Prescribed Fire	1	170100	0.000149	0.7	0.75	0.75
Alluvial	Shrub Low Severity Fire	1	170100	0.000149	0.5	0.7	0.7
Alluvial	Shrub Moderate Severity Fire	1	170100	0.000149	0.3	0.5	0.5
Alluvial	Shrub High Severity Fire	1	948600	0.0004343	0.05	0.25	0.25
Alluvial	Bare Slope	1	750000	0.004	0.05	0.2	0.2
Alluvial	Sod Grass	1	196700	0.0004446	0.4	0.6	0.6
Alluvial	Bunch Grass	1	196700	0.0004446	0.6	0.8	0.8

Volcanic	Old Forest	1.5	300000	0.00005	0.9	1	1
Volcanic	Young Forest	1.5	600000	0.0001	0.8	1	1
Volcanic	Forest Thinning 96% cover	1.5	600000	0.00002	0.4	0.96	0.96
Volcanic	Forest Thinning 93% cover	1.5	600000	0.00002	0.4	0.93	0.93
Volcanic	Forest Thinning 85% cover	1.5	600000	0.00002	0.4	0.85	0.85
Volcanic	Forest Prescribed Fire	1.5	1000000	0.0002	0.85	0.85	0.85
Volcanic	Forest Low Severity Fire	1.5	1000000	0.0002	0.75	0.8	0.8
Volcanic	Forest Moderate Severity Fire	1.5	1000000	0.0002	0.4	0.5	0.5
Volcanic	Forest High Severity Fire	1.5	1500000	0.0003	0.2	0.3	0.3
Volcanic	Shrubs	1.5	134500	0.0000846	0.7	0.9	0.9
Volcanic	Shrub Prescribed Fire	1.5	162200	0.0001444	0.7	0.75	0.75
Volcanic	Shrub Low Severity Fire	1.5	162200	0.0001444	0.5	0.7	0.7
Volcanic	Shrub Moderate Severity Fire	1.5	162200	0.0001444	0.3	0.5	0.5
Volcanic	Shrub High Severity Fire	1.5	904400	0.0004209	0.05	0.3	0.3
Volcanic	Bare Slope	1.5	600000	0.003	0.05	0.2	0.2
Volcanic	Sod Grass	1.5	187600	0.0004309	0.4	0.6	0.6
Volcanic	Bunch Grass	1.5	187600	0.0004309	0.6	0.8	0.8

Basin-scale statistical analyses

Management scenario comparison

After running the WEPPcloud interface for all watersheds in the basin, and for all 11 conditions, we saved the model outputs, including information regarding elevation, slope, aspect, soil properties, landuse, etc. for each modeled hillslope as shapefiles and tables. We further plotted the data and performed calculations and statistical analyses to compare soil erosion between the different management conditions as well as to better understand the drivers for sediment and phosphorus yield.

To compare the potential soil erosion changes from the management scenarios we calculated annual average sediment yield by each treatment. A histogram of the data indicates that non-zero sediment yield are highly skewed and appear to fit a log normal distribution (Fig. 3). Therefore, this analysis used the data filtered to non-zero sediment yield, as zero values within a dataset make linear modelling difficult. Additionally, only observations with non-zero sediment yield are informative. Since we are only using a subset of the data, this is a conditional analysis.

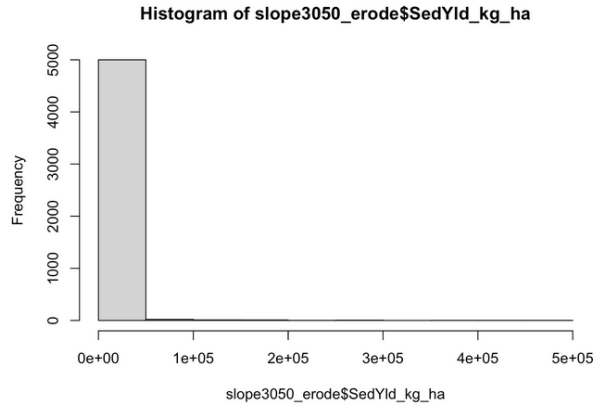

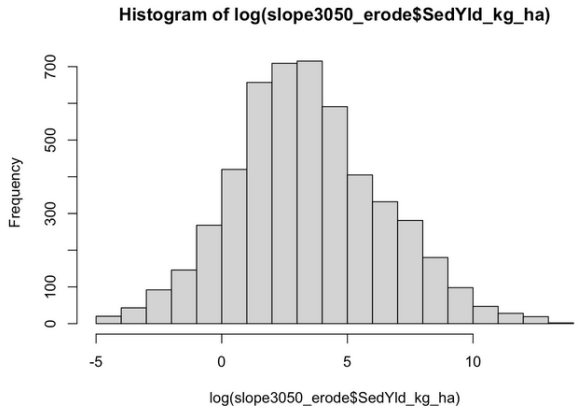

Fig. 3. Histogram of sediment yield for hillslopes between 30-50% that erode. Untransformed data (left) and log-transformed data (right).

Estimating Treatment Benefits

One approach to evaluating the impacts of thinning is to compare the erosion associated with thinning as an absolute difference in sediment yield from thinning as compared to current conditions by hillslope (Eq. 1). These calculations were performed on the hillslope output data and then mapped for the Blackwood Watershed, which we used as an example. For all these calculations we used the thinning scenario with the 85% post-treatment ground cover. Since post-thinning ground cover in Lake Tahoe Basin often exceeds 85% (Norman et al., 2008, Pell and Gross, 2016, Christensen and Norman, 2007), we consider the thin 85% a worst-case thinning scenario.

Eq. 1

$$AbsoluteDifference = Thinning85cover - CurrentErosion$$

Thinning forested hillslopes can reduce fire severity. However, thinning can also increase erosion compared to undisturbed or current conditions. We estimated a treatment benefit based on four of the modeled conditions (unburned, thin 85%, low severity and moderate severity). The estimated erosion rates would generally occur in the year of the disturbance. Most forested watersheds recover quickly from disturbances associated with low severity fire or thinning. We selected the thinning scenario with the most post-disturbance ground cover (85% cover) and assumed that by thinning, the burn severity would be reduced from a moderate severity to the low severity. We also assumed that thinning would be carried out three times as often as a wildfire would occur, for example every 20 years for thinning instead of every 60 years for wildfire. We selected a thinning regime of 20 years because it is common practice in the basin; however, we also tested treatment benefits by thinning 1, 10, 20, 30, 40, 50, and 60 times within the 60 years fire return interval.

We then defined and calculated the Treatment Benefit as:

Eq. 2

$$TreatmentBenefit = (ModerateSeverity - LowSeverity) - ((Thinning85 - CurrentConditions)x3)$$

Treatment effects on sediment yield for slopes 30–50%

Specifically, we were interested in sediment and phosphorus yield following thinning on steeper slopes (30–50%) since these hillslopes are now considered for mechanical thinning by managers looking to reduce ground fuels to minimize wildfire risks.

We further tested the change in probability of eroding versus not eroding for different treatments. We accomplished this by calculating odds ratios and risk ratios, for all hillslopes with sediment yield > 0 kg/ha and between 30–50% slopes. In this analysis, we only considered three thinning scenarios, the prescribed fire scenario, and the high severity wildfire scenario as a worst-case scenario. The *odds ratio* indicates the change of odds of erosion versus no erosion under current conditions compared to

the other treatments. The *risk ratio*, slightly different from the odds ratio, calculates the risk of erosion for the entire population of each scenario. Like the odds ratio, it is comparing the ratio between the reference level, current conditions, fire, and thinning scenarios. The results are otherwise interpreted the same as an odds ratio.

Lastly, we ran a *Generalized Linear Model* (GLM) of scenario versus sediment yield using a log-normal distribution The results of the Analysis of Variance (ANOVA) are presented along with pairwise comparison between each treatment and the current conditions (which is treated as a reference level in the analysis).

Variable importance

In addition to the data analysis presented so far, we also performed several exploratory data analyses such as Correlations, Principal Component Analysis (PCA)**,** and Random Forest (RF). These analyses were performed on various environmental variables extracted by hillslope from the WEPP model input data.

Correlations, specifically spearman correlations, were performed by first considering all the forested hillslopes in the basin, and then by some of the most eroding forested watersheds (i.e. Blackwood Creek, Ward Creek, Trout, and Upper Truckee). All correlations were performed with the statistical software R with the package *psych* at $\alpha \leq 0.001$.

PCA is a multivariate statistical data analysis that is used to reduce a large number of correlated variables into uncorrelated variables, named principal components, and to infer underlying relationships between the set of variables. In general, PCA provides an understanding of:

1. The relationship between the variables;
2. The direction in which data are dispersed; and
3. The relative importance of each direction.

Variables that point in the same direction are positively correlated while those that point in opposite directions are negatively correlated. Variables that are perpendicular are not correlated.

We used a PCA analysis to explore the distribution of sediment yield relative to several soil and topographical variables. For displaying purposes, a categorical variable *SedYld_Class* was created by binning sediment yield into 3 categories: no erosion, low erosion, and high erosion. The cutoff between low erosion and high erosion categories was set to split the data in relatively equal parts. We created PCA plots based on the forested hillslopes for each management condition.

RF or random decision forest is a type of machine learning algorithm used for classification or regression of multiple variables within a dataset. We used the RF algorithms to predict if a hillslope will erode or not and also to predict the hillslope sediment yield for current conditions, 85% thinning, prescribed fire, and high severity fire based on multiple physical attributes. The "observed" sediment yield in this case was the WEPP modeled sediment yield at each hillslopes. While this approach is redundant (i.e. predicting soil erosion already predicted by WEPP), we were mainly interesting in identifying physical hillslope attributes that explain the variability in soil erosion.

To predict if a hillslope will erode or not, we created a new variable *SedVar* by converting sediment yield to a binary variable where any data point greater than zero was classified as "eroded" and all data points equal to zero were classified as "non-eroded". To predict the actual values of sediment yield, we used the WEPP-predicted sediment yield resulted from the four management scenarios: current conditions, thinning 85%, prescribed fire, and high severity fire.

IV. RESULTS AND DISCUSSION

Model performance assessment

Streamflow and water yield assessment

The WEPP model was applied to 17 watersheds of varying sizes in the Lake Tahoe Basin. The overall goodness-of-fit statistics for the WEPP-simulated and observed daily streamflow comparisons for the watersheds indicate reasonable results (Table 4). Across the watersheds, *NSEs* based on daily streamflow values were in the range of 0.44 to 0.64 indicating satisfactory agreement between modeled and observed values. The only exception was the Logan House Creek watershed (LH1), located on the eastern side of the Lake Tahoe Basin, with an *NSE* of −0.09 signifying poor model performance. Brooks et al. (2016) reported similar results for the LH1 watershed, which the authors attributed to water loss through fractures in the bedrock. The WEPP model was not able to simulate this complex hydrogeology without additional calibration. Positive *KGE* values in the range of 0.56 to 0.78 (excluding watershed LH1) suggest reasonable model performance when considering mean flow as a *KGE* estimation criterion. *Pbias* within ± 3.81% across all watersheds indicated slight over- and under-prediction of streamflow (Table 4).

The WEPP model captured runoff regimes across all watersheds reasonably well, and the simulated annual trends of water yield followed the trends of observed yield (Fig. 4 and 5). Compared to daily streamflow, monthly and annual goodness-of-fit statistics showed improved model performance for all watersheds (Table 4).

Table 4. Goodness-of-fit statistics for observed and simulated streamflow simulations. D = daily, M = monthly, A = annually (Water Year) statistics.

No.	Name	Begin	End	*NSE*			*KGE*			*PBias (%)*		
				D	***M***	***A***	***D***	***M***	***A***	***D***	***M***	***A***
						California						
1	WC8	1/1/1990	9/30/2014	0.59	0.69	0.94	0.60	0.72	0.84	4.5	4.8	4.5
2	WC7A	10/1/1991	9/30/2001	0.59	0.71	0.98	0.62	0.77	0.92	0.3	0.4	0.3
3	WC3A	10/1/1991	11/1/2011	0.61	0.71	0.96	0.65	0.73	0.94	0.3	0.5	0.3
4	BC1	1/1/1990	9/30/2014	0.59	0.66	0.94	0.61	0.69	0.85	0.1	0.3	0.1
5	GC1	1/1/1990	9/30/2014	0.54	0.61	0.90	0.66	0.71	0.89	10.7	11	10.7
6	UTR1	1/1/1990	9/30/2014	0.53	0.63	0.91	0.73	0.78	0.86	12.8	13.1	12.8
7	UTR3	6/1/1990	9/30/2012	0.56	0.66	0.96	0.77	0.82	0.9	6.3	6.4	6.3
8	UTR5	5/12/1990	10/11/2011	0.59	0.73	0.93	0.78	0.83	0.84	−7.7	−7.8	−7.7
9	TC4	1/1/1990	9/30/2014	0.64	0.69	0.86	0.75	0.77	0.74	−9.9	−9.8	−9.9
10	TC2	6/1/1990	9/30/2012	0.54	0.60	0.92	0.77	0.79	0.84	−6.8	−6.8	−6.8
11	TC3	5/22/1990	3/31/2011	0.48	0.53	0.87	0.67	0.69	0.76	0.3	0.3	0.3
						Nevada						
12	LH1	1/1/1990	10/12/2011	−0.09	0.49	0.77	0.39	0.48	0.62	−3.2	−3.1	−3.2
13	GL1	1/1/1990	9/30/2012	0.53	0.66	0.87	0.56	0.60	0.77	2.8	2.8	2.8
14	IN1	1/1/1990	9/30/2014	0.44	0.57	0.72	0.56	0.56	0.60	−3.2	−3.2	−3.2
15	IN2	1/1/1990	9/30/2004	0.48	0.65	0.81	0.62	0.61	0.70	−2.2	−2.2	−2.2
16	IN3	5/1/1990	3/31/2011	0.48	0.71	0.80	0.69	0.66	0.68	−1.5	−1.4	−1.5
17	TH1	1/1/1990	9/30/2014	0.60	0.82	0.86	0.76	0.89	0.87	0	−0.1	0
	Mean[§]			**0.55**	**0.66**	**0.89**	**0.68**	**0.73**	**0.81**	**3.81**	**1.40**	**3.81**

[§] *Mean values calculated without LH1 watershed.*

See Fig. 1 for watershed location and Table A1 in Appendix for full watershed names.

Nevertheless, uncalibrated model results in this study suggest that the WEPPcloud interface can satisfactorily represent the hydrology of distinct geographic regions and that water resources managers could apply the interface to ungauged watersheds for forest management decisions. Future efforts to improve hydrologic simulations with the WEPPcloud interface are underway to improve the snow hydrology routines in WEPP.

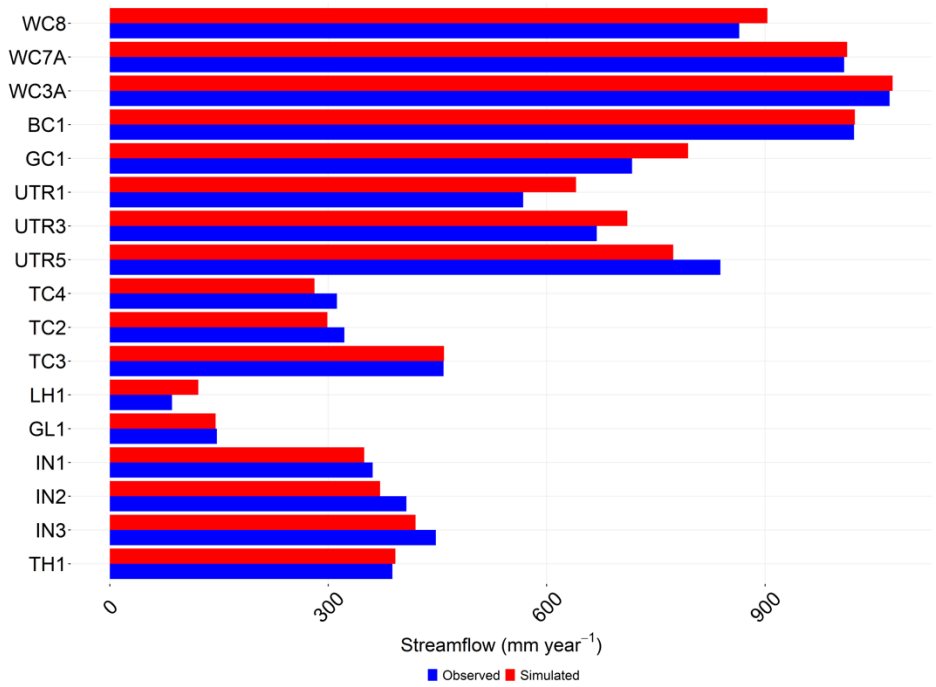

Fig. 4. Comparison of observed and simulated average annual water yield for the study watersheds.

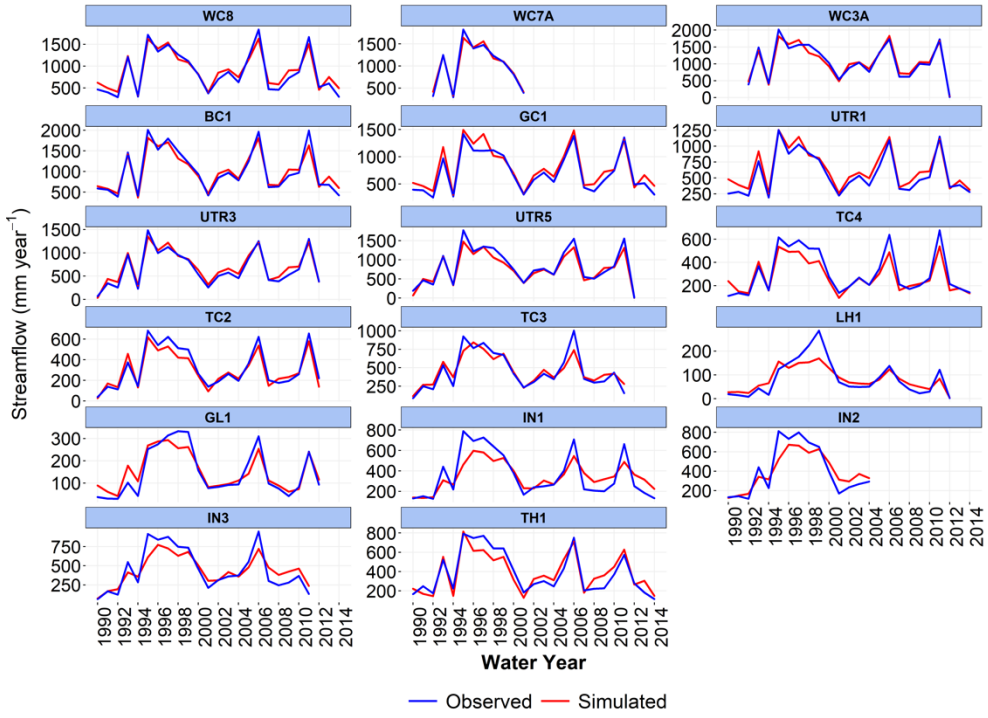

Fig. 5. Comparison of simulated and observed annual streamflow.

A linear groundwater reservoir with a default k_b of 0.04 d^{-1} was appropriate to model low summer streamflow in most watersheds of this study, except in the drier watersheds on the east-side of the

basin. For these watersheds, the initial model results showed overestimations in water yield. Similar results were reported by Brooks et al. (2016) in Logan House (LH1) and Glenbrook Creek (GC1) watersheds. In their study, the authors used a secondary reservoir to simulate water yield by allowing groundwater loss through hydrogeological fractures and, therefore, bypassing the USGS stream gauge. In this study, the addition of a second aquifer reservoir in nine watersheds located in the NE, E, and SE of the Lake improved water yield simulations, supporting an okd hypothesis that these watersheds could be characterized by complex hydrogeology (Hyne et al., 1972). Calibrated k_b and k_s for all watersheds are shown in Table 5.

Table 5. Calibrated parameter values for baseflow and deep seepage coefficients, channel critical shear stress, and phosphorus concentrations in surface runoff, subsurface lateral flow, baseflow, and sediment.

No.	Name	Baseflow coefficient (d^{-1})	Deep seepage coefficient (d^{-1})	τ_c (Nm^{-2})	P_{runoff} (mg L^{-1})	$P_{lateral}$ (mg L^{-1})	$P_{baseflow}$ (mg L^{-1})	$P_{sediment}$ (mg L^{-1})
				California				
1	WC8	0.04	0	30	0.004	0.005	0.006	1300
2	WC7A	0.04	0	30	0.005	0.006	0.007	1100
3	WC3A	0.04	0	30	0.003	0.004	0.005	900
4	BC1	0.04	0	10	0.003	0.004	0.005	1100
5	GC1	0.04	0	45	0.002	0.003	0.004	1300
6	UTR1	0.04	0	15	0.004	0.005	0.006	1200
7	UTR3	0.04	0	70	0.003	0.004	0.005	1300
8	UTR5	0.04	0	180	0.007	0.008	0.009	1300
9	TC4	0.01	0.0062	45	0.008	0.009	0.010	1800
10	TC2	0.0168	0.0105	45	0.008	0.009	0.010	1700
11	TC3	0.01	0.0010	75	0.007	0.008	0.009	1500
				Nevada				
12	LH1	0.0005	0.0009	40	0.001	0.002	0.003	2500
13	GL1	0.0018	0.0016	35	0.015	0.016	0.017	3500
14	IN1	0.0019	0.0010	35	0.011	0.012	0.013	1500
15	IN2	0.0017	0.0006	40	0.011	0.012	0.013	1300
16	IN3	0.0022	0.0009	45	0.010	0.011	0.012	1300
17	TH1	0.0130	0.0134	25	0.008	0.009	0.010	700

See Fig. 1 for watershed location and Table A1 in Appendix for full watershed names.

Sediment load

Observed annual average sediment loads generally varied between the west- and the east-side, and from watershed to watershed. Eastern watersheds generated considerably less sediment compared to watersheds from the western side of the basin. Observed annual average sediment loads ranged from 5 Mg yr^{-1} at Logan House Creek (LH1) to 2852 Mg yr^{-1} from Blackwood Creek (BC1). This difference is mainly due to differences in area and precipitation since the LH1 watershed received less than half of the precipitation recorded in the BC1 (657 mm yr^{-1} precipitation in LH1 compared to 1476 mm yr^{-1} recorded in BC1; Table 2). Other watershed characteristics such as watershed soils, geology, and vegetation, may also contribute to the difference in sediment loads between the two watersheds, albeit to a lesser extent.

Model results showed an underestimation of annual sediment loads at three watersheds in the western side of the basin, namely at Blackwood Creek (BC1), Ward Creek (WC8), and General Creek (GC1) (Figs. 6 and 7). The main reason for this underestimation was due to sediment delivery associated with a few high peak flow events from 1 and 2 January 1997 (WY 1997) and on 31 December 2005 (WY 2006), which were not captured by the model. These high peak flow rates were caused by rain-on-snow events that are often observed in the mid-winter in Pacific Northwest (Marks et al., 2001) and in watersheds in the Sierra Nevada mountains (Kattelmann, 1997; McCabe et al., 2007). In the Lake Tahoe Basin, the 1997 event was considered a 100-year flood event (Tetra Tech, 2007), which caused peak suspended sediment loads with return periods ranging from 40 to 60 years only in streams from the western side of Lake Tahoe (Simon et al., 2004). Brooks et al. (2016) demonstrated that the WEPP model can accurately simulate the 1997 high peak flow in the Upper Truckee River (UTR5) when scaling the weather data across the watershed based on data from a lower elevation SNOTEL station, which recorded a slightly different rain distribution for the day. Since most of the sediment is delivered during these high peak flow events, an accurate representation of weather data is essential to model such events.

Another potential source of underestimation of sediment load by WEPP may be sediment delivery from landslides, as the WEPP model does not consider mass wasting sources of sediment. There is some evidence of mass wasting, particularly in the steeper upland portions of the Blackwood Creek (BC1) watershed (Gavigan, 2007). Additional sediment during peak flows may also be from channel erosion processes not addressed by the WEPP model, like side sloughing during channel drawdown following flood flows that would have saturated the stream banks (Simon et al. 2009).

The goodness-of-fit statistics based on annual sediment loads for all simulated years show that WEPP predictions were in reasonable agreement with observed data except for WC8, BC1, and GC1 watersheds (Table 6). Results for the three watersheds improved substantially when the water years with high peak flow events (1997 and 2006) were omitted from the analysis. For example, *NSE*, *KGE*, and *Pbias* for watershed BC1 improved from 0.05 to 0.63, −0.15 to 0.48, and −60% to −7%, respectively.

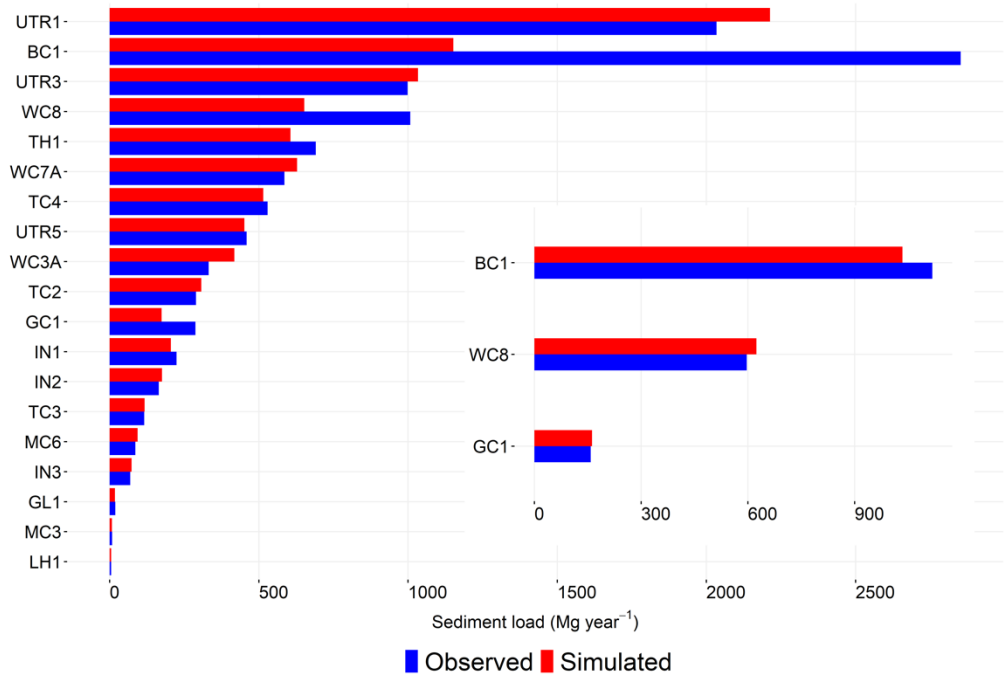

Fig. 6. Comparison of WEPP-simulated and observed average annual sediment load. WEPP underestimated sediment loads in the three watersheds (WC8, BC1, and GC1) that were affected by the rain-on-snow events in WY 1997 and 2006. The inset figure shows WEPP-simulated and observed sediment load after excluding these two years.

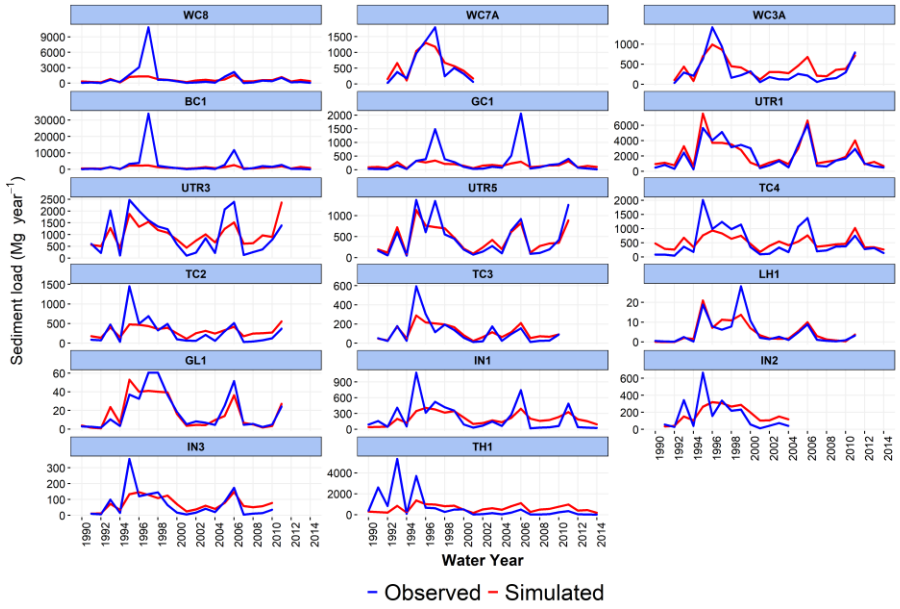

Fig. 7. Comparison of WEPP-simulated and observed annual sediment load.

Table 6. Goodness-of-fit statistics for the WEPP-simulated and observed annual sediment load. Italicized rows denote watersheds where statistics were recalculated after eliminating sediment load in 1997 and/or 2006 water years that experienced high peak flow events and extreme soil erosion.

No.	*Name*	*nPairs*	*NSE*	*KGE*	*PBias (%)*
			California		
1	WC8	25	0.16	0.03	–35.3
1	*WC8*[†]	*25*	*0.62*	*0.48*	*4.6*
2	WC7A	10	0.78	0.70	7.2
3	WC3A	20	0.67	0.60	26
4	BC1	25	0.05	–0.15	–59.6
4	*BC1*[††]	*25*	*0.63*	*0.48*	*–7.2*
5	GC1	25	0.15	0.03	–39.4
5	*GC1*[††]	*25*	*0.58*	*0.49*	*1.9*
6	UTR1	25	0.82	0.88	8.8
7	UTR3	21	0.60	0.56	3.5
8	UTR5	21	0.80	0.70	–1.7
9	TC4	25	0.47	0.38	–2.8
10	TC2	21	0.41	0.32	6.1
11	TC3	20	0.65	0.53	0.9
			Nevada		
12	LH1	22	0.73	0.74	–2.2
13	GL1	22	0.79	0.81	–6.6
14	IN1	25	0.43	0.36	–8.3
15	IN2	14	0.36	0.39	6.4
16	IN3	20	0.51	0.45	7.2
17	TH1	25	0.12	0.02	–12.4
	Mean[§]		**0.59**	**0.52**	**5.95**

[†] *Calculations without WY 1997.*
[††] *Calculations without WY 1997 and 2006.*
[§] *Mean values calculated without WY 1997 and WY 2006 for WC8, BC1, and GC1.*
See Fig. 1 for watershed location and Table A1 in Appendix for full watershed names.

We manually calibrated the τ_c in the Lake Tahoe watersheds to match the simulated to observed annual sediment loads at the watershed outlets, assuming minimal upland erosion. These values ranged from 10 Nm^{-2} in the Blackwood Creek watershed to 180 Nm^{-2} in the headwaters of the Upper Truckee River (UTR5) watershed (Table 5). Lower values of the τ_c are associated with smaller D_{50} particle size (Srivastava et al., 2020), and therefore higher soil erodibility for channel beds. Conversely, higher values of τ_c are associated with larger D_{50} particle sizes and result in lower erodibility values. Indeed, the Blackwood Creek watershed is known in the Lake Tahoe Basin as the top contributor of sediment yield to the lake and has been the subject of several channel restoration efforts (Norman et al., 2014; Oehrli, 2013). The headwater portion of the Upper Truckee River watershed is characterized by rock outcrops of low infiltration rates and erodibilities (Brooks et al., 2016), which can be an explanation for the higher τ_c calibrated by the model. Median pebble count data (D_{50}) was available for two of the modeled watersheds in the Lake Tahoe Basin and τ_c equivalents for these two watersheds approximately matched the calibrated values $\tau_{c\text{-calibrated}}$: Blackwood Creek, mainstream, D_{50} = 42, τ_c = 26, $\tau_{c\text{-calibrated}}$ = 10; Ward Creek, D_{50} = 68 τ_c = 54, $\tau_{c\text{-calibrated}}$ = 30.

Phosphorus yield

The magnitudes of all three phosphorus constituents simulated by the WEPP model were in close agreement with the observed across all watersheds (Figs. 8a and 8b). The goodness-of-fit statistics based on annual values were very good for all three phosphorus constituents (Table 7): TP (*NSE* = 0.75, *KGE* = 0.71, *PBias* = −0.5%), PP (*NSE* = 0.71, *KGE* = 0.70, *PBias* = −1.3%), and SRP (*NSE* = 0.66, *KGE* = 0.66, *PBias* = −4.6%). The simulated annual loads of TP, PP, and SRP followed the trends of observed load (data not shown), which is expected since PP, which is transported mainly with sediments, is the major form of phosphorus transport in streams from Lake Tahoe (Hatch et al., 2001). Therefore, similar to the sediment load, the TP and PP load for the three watersheds (WC8, BC1, and GC1) that experienced the rain-on-snow events in WY 1997 and 2006 were also underestimated (Figure 8a). Simulated annual SRP load was better captured by the model, except in Logan House (LH1) where the model underestimated the observed loads (*PBias* = −95%; Table 7). However, it is worth noting that the difference between the observed and simulated phosphorus load for this watershed is insignificant (1.5 kg yr^{-1}).

The simplistic coefficient-based phosphorus algorithms implemented in the WEPPcloud interface were sufficient to capture the general trends of annual phosphorus loads associated with surface runoff, subsurface lateral flow, baseflow, and sediment in our study watersheds (Figs. 8 and 9). Most process-based phosphorus models use complex processes involving mineralization, decomposition, and immobilization pools and their interaction among them for phosphorus transport computations. Hydrologic simulations with such algorithms may improve the spatial and temporal estimates of phosphorus for watershed simulation studies. A version of the WEPP model with a water quality module is under development (personal communication, D.C. Flanagan) and would likely be available for the evaluation of nutrient transport in forest settings in the future version of WEPPcloud.

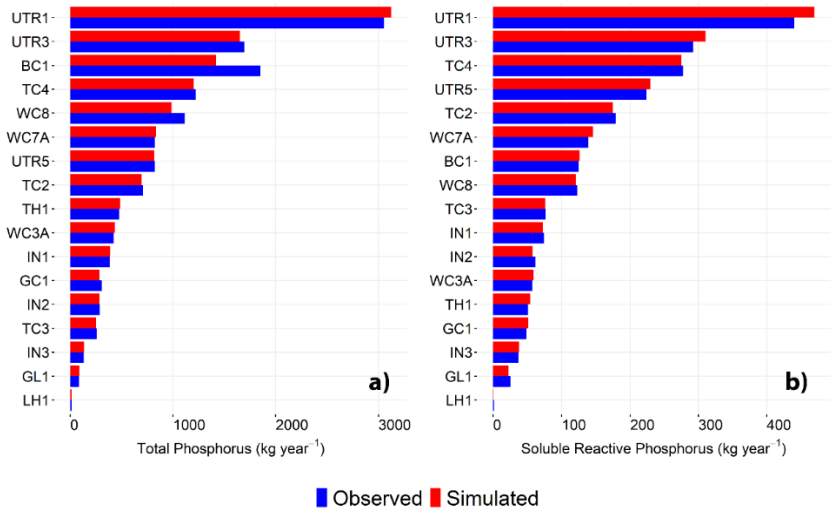

Fig. 8. Comparison of WEPP-simulated and observed average annual TP (a) and SRP (b) loads. PP exhibited similar trends as TP.

Table 7. Goodness-of-fit statistics for the average annual phosphorus load for the three constituents (TP = Total Phosphorus, PP = Particulate Phosphorus, and SRP = Soluble Reactive Phosphorus). Italicized rows denote watersheds where statistics were recalculated after eliminating phosphorus load in 1997 and/or 2006 water years that experienced high peak flow events and extreme soil erosion.

No.	Name		TP			PP			SRP		
		nPairs	*NSE*	*KGE*	*Pbias (%)*	*NSE*	*KGE*	*Pbias (%)*	*NSE*	*KGE*	*Pbias (%)*
						California					
1	WC8	25	0.56	0.43	–11.5	0.53	0.41	–12.7	0.83	0.70	–2.2
1	*WC8*[†]	*25*	*0.79*	*0.65*	*2.5*	*0.77*	*0.71*	*2.6*	*0.83*	*0.71*	*0.6*
2	WC7A	20	0.94	0.96	1.6	0.93	0.96	0.8	0.94	0.91	5
3	WC3A	10	0.75	0.82	2.8	0.75	0.83	2.3	0.64	0.66	3.9
4	BC1	25	0.39	0.28	–23.3	0.37	0.25	–25.2	0.69	0.67	1.2
4	*BC1*[††]	*25*	*0.70*	*0.63*	*0.4*	*0.69*	*0.62*	*0.3*	*0.69*	*0.62*	*0.5*
5	GC1	25	0.64	0.53	–8	0.57	0.46	–11	0.75	0.84	6.2
5	*GC1*[††]	*25*	*0.79*	*0.74*	*4.1*	*0.75*	*0.82*	*3.3*	*0.74*	*0.82*	*6.1*
6	UTR1	25	0.81	0.85	2.3	0.75	0.78	1.5	0.8	0.68	6.6
7	UTR3	21	0.83	0.71	–2.4	0.79	0.70	–4.3	0.77	0.69	6.3
8	UTR5	21	0.86	0.83	–0.7	0.76	0.77	–2	0.94	0.89	2.5
9	TC4	25	0.80	0.65	–1.6	0.75	0.61	–1.8	0.87	0.76	–0.9
10	TC2	21	0.70	0.55	–1.6	0.59	0.47	–1.5	0.9	0.79	–2.4
11	TC3	20	0.84	0.83	–3.3	0.81	0.81	–4.6	0.89	0.83	–0.8
						Nevada					
12	LH1	22	0.63	0.68	–21.9	0.53	0.64	–28.6	–1.17	-0.39	–94.6
13	GL1	22	0.83	0.91	3	0.75	0.81	2.3	0.77	0.79	–10.9
14	IN1	25	0.65	0.58	1.2	0.64	0.58	2.1	0.64	0.49	–2.3
15	IN2	14	0.59	0.59	–0.8	0.56	0.59	0.9	0.66	0.54	–6.2
16	IN3	20	0.82	0.79	3	0.80	0.82	2.4	0.56	0.65	2.5
17	TH1	25	0.41	0.36	2.7	0.37	0.33	1.9	0.75	0.83	5.7
	Mean[§]		**0.75**	**0.71**	**–0.51**	**0.71**	**0.70**	**–1.32**	**0.66**	**0.66**	**–4.61**

[†] *Calculations without WY 1997.*

[††] *Calculations without WY 1997 and 2006.*

[§] *Mean values calculated without WY 1997 and WY 2006 for WC8, BC1, and GC1.*

See Fig. 1 for watershed location and Table A1 in Appendix for full watershed names.

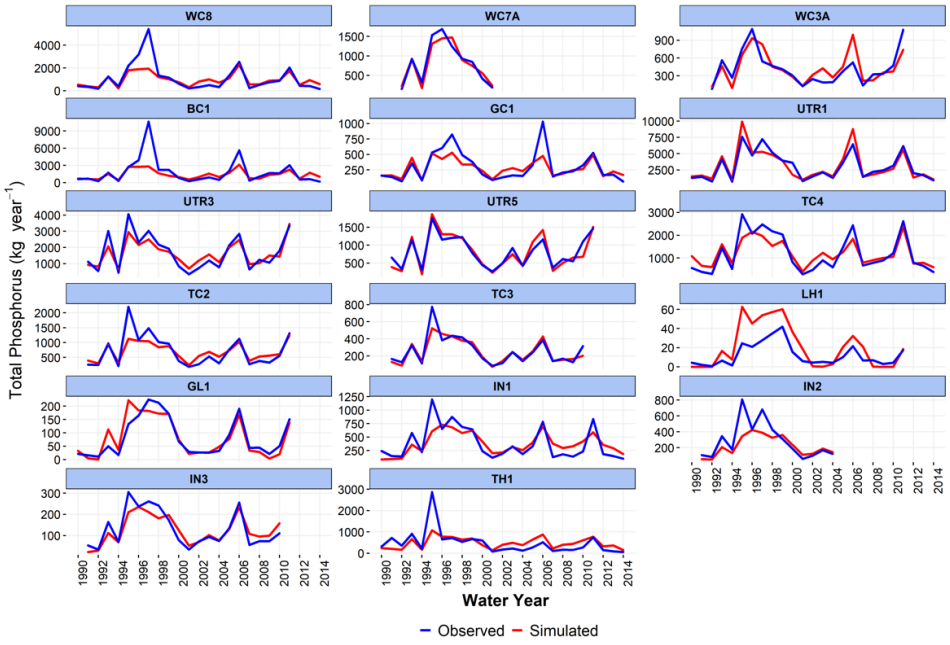

Fig. 9. Comparison of WEPP-simulated and observed annual TP loads for the Lake Tahoe Basin watersheds. SRP and PP exhibited similar trends as TP.

Phosphorus concentration values in runoff inferred from the observed data varied between 0.0028 mg L^{-1} in General Creek (GC1) to 0.013 mg L^{-1} in Glenbrook Creek (GL1). The lateral flow and baseflow P concentrations were higher than those in the runoff and ranged between 0.026 mg L^{-1} in Logan House (LH1) to 0.0153 mg L^{-1} in Glenbrook Creek (GL1) for lateral flow, and from 0.0024 mg L^{-1} in Logan House (LH1) to 0.0228 mg L^{-1} in Glenbrook Creek (GL1) for baseflow, respectively. In general, these values were lower in watersheds located on the western side and higher in those from the eastern side of the basin. The observed P concentrations in the sediments varied between 840 mg kg^{-1} in Third Creek (TH1) to 4397 mg kg^{-1} in Glenbrook Creek (GL1). Similarly, as with the streamflow P concentrations, sediment P concentrations varied among watersheds, with lower values in watersheds on the northern, western, and southern sides of the basin and higher values in watersheds from the eastern side of the basin (Table 8).

The significant difference in P concentration in runoff and sediment between watersheds on the west- and east sides of Lake Tahoe, respectively, is likely due to differences in the parent material. Specifically, watersheds located on the NW and W of Lake Tahoe are mainly underlying volcanic soils with poorly crystalline iron and aluminum oxides that retain P and limit the P movement in water (Heron et al., 2020). Watersheds on the eastern side of the Lake Tahoe Basin, however, are developed mainly on granitic parent material with greater potential for P mobilization to streamflow (Heron et al., 2020).

Table 8. Observed (Obs.) and calibrated (Calib.) phosphorus concentrations. Observed values are inferred from the flow-weighted phosphorus and sediment concentrations calculated with the LOADEST model.

No.	Name	Single/ Double aquifer reservoir	Obs. in runoff (mg L^{-1})	Calib. in runoff (mg L^{-1})	Obs. in lateral flow (mg L^{-1})	Calib. in lateral flow (mg L^{-1})	Obs. in baseflow (mg L^{-1})	Calib. in baseflow (mg L^{-1})	Obs. in sediment (mg kg^{-1})	Calib. in sediment (mg kg^{-1})
					California					
1	WC8	Single	0.0059	0.004	0.009	0.005	0.0125	0.006	2059	1300
2	WC7A	Single	0.0053	0.005	0.009	0.006	0.0147	0.007	1188	1100
3	WC3A	Single	0.0034	0.003	0.004	0.004	0.0045	0.005	1600	900
4	BC1	Single	0.0040	0.003	0.007	0.004	0.0116	0.005	1166	1100
5	GC1	Single	0.0028	0.002	0.009	0.003	0.0187	0.004	1303	1300
6	UTR1	Single	0.0049	0.004	0.006	0.005	0.0070	0.006	1362	1200
7	UTR3	Single	0.0034	0.003	0.004	0.004	0.0050	0.005	1896	1300
8	UTR5	Single	0.0052	0.007	0.010	0.008	0.0209	0.009	2466	1300
9	TC4	Double	0.0073	0.008	0.008	0.009	0.0094	0.01	2966	1800
10	TC2	Double	0.0080	0.008	0.009	0.009	0.0099	0.01	1789	1700
11	TC3	Double	0.0077	0.007	0.009	0.008	0.0104	0.009	2545	1500
					Nevada					
12	LH1	Double	0.0037	0.002	0.003	0.003	0.0024	0.004	3875	2300
13	GL1	Double	0.0130	0.015	0.015	0.016	0.0228	0.017	4397	3500
14	IN1	Double	0.0109	0.011	0.012	0.012	0.0141	0.013	1727	1500
15	IN2	Double	0.0123	0.011	0.012	0.012	0.0120	0.013	1248	1300
16	IN3	Double	0.0104	0.01	0.011	0.011	0.0127	0.012	2280	1300
17	TH1	Double	0.0080	0.008	0.011	0.009	0.0138	0.01	840	700
	Mean	**Single**	**0.004**	**0.004**	**0.007**	**0.005**	**0.012**	**0.006**	**1630**	**1188**
	Mean	**Double**	**0.009**	**0.009**	**0.010**	**0.010**	**0.012**	**0.011**	**2407**	**1733**

Observed in runoff: Average SRP concentrations for April and May.
Observed in lateral flow: Average SRP concentrations of all months, except April, May, September, and October.
Observed in baseflow: Average SRP concentrations for September and October.
Observed in sediment: Average (TP-SRP) x 10^6 /SSC for May.
See Fig. 1 for watershed location and Table A1 in Appendix for full watershed names.

Basin-scale model runs

The model calibration for the 17 watersheds in the basin allowed us to identify the minimum number of critical calibrating parameters in the model to confidently simulate streamflow, and sediment and phosphorus yield. Model results suggested that most of the calibrated parameters are fairly consistent across each ecosystem where a calibrated value in one watershed is also reasonable for a neighboring watershed in the same ecosystem. For example, eight watersheds in the western side of the basin were calibrated with a single linear reservoir aquifer and a baseflow recession coefficient of 0.04 day^{-1}. Conversely, all watersheds located NE, E, and SE were calibrated with a second linear reservoir and various deep seepage coefficients. These similarities among watersheds allowed us to apply the calibrated values to model the rest of the ungauged watersheds within the basin. Regional differences were also observed for the channel critical shear and phosphorus concentrations, which were similarly distributed across the basin (Figs A1, A2, A3).

WEPPcloud simulated output can be downloaded as summarized tables and GIS shapefiles (Fig. 10) and managers can use this information to compare runoff, sediment yield, and phosphorus yields from individual hillslopes and watersheds (https://wepp.cloud/weppcloud/lt/). For example, maps of sediment yield output suggest that under undisturbed conditions there are erosion hot spots within several watersheds in the basin (e.g. Blackwood Creek, Ward Creek, upland portion of the Upper Truckee River, and Third Creek) and that sediment yield from these areas tends to increase with disturbance severity (Fig. 11). Another observation with great implications for management is that for the eastern watersheds, the model simulated minimal to no erosion even after a wildfire (< 1 kg ha^{-1}). Two of the eastern watersheds have been identified in previous research studies as sinks, rather than sources of sediments mainly due to their small size and low precipitation and runoff rates (Simon et al., 2004). This finding could be useful to prioritize areas for treatment in the basin.

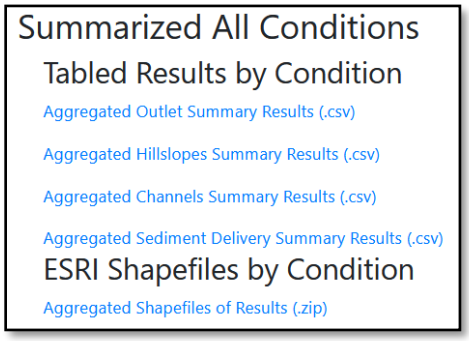

Fig. 10. Summarized results for all watersheds in the Lake Tahoe available on the WEPPcloud interface.

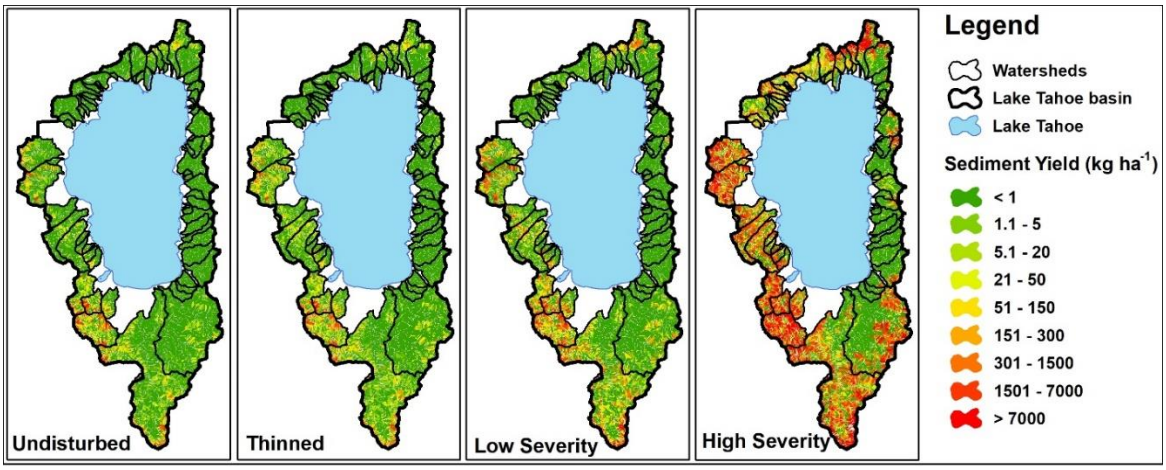

Fig. 11. Annual average sediment delivery rate for four scenarios: undisturbed, thinned, uniform low severity fire, and uniform high severity fire. Similar maps can be created from the model results for other hydrologic components (e.g. runoff, lateral flow, baseflow) or scenarios (e.g. uniform prescribed fire, uniform moderate severity fire, based on future climate scenarios, etc.).

Previous research in the basin suggested that high peak flows associated with rain-on-snow events (e.g., year 1997) can flush stored sediment from the stream channels and reduce the sediment load in the following years (Simon et al., 2004). Since forest disturbances have the potential to increase peak

flows (Grant et al., 2008), we could expect rill and interrill erodibilities and the channel critical shear to change immediately post-disturbance. However, without clear guidelines from the available literature, we were unable to parameterize the WEPPcloud interface to reflect these complex changes within the channel streambed post-disturbance.

Similarly, forest treatments and wildfire have the potential to increase P concentrations in forested ecosystems mainly through increases in soil erosion and increased availability of ash (Santín et al., 2018). However, studies have found little effects from thinning (Deval et al., 2021) or from a combination of thinning and prescribed fires on P delivery (Kaye et al., 2005; Martin and Harr, 1989). Since forest wildfires, especially those that result in high soil burn severity, affect soil properties, there is more evidence that P concentrations post-wildfire increase (Lane et al., 2008; Murphy et al., 2006; Santín et al., 2018; Smith et al., 2011). However, because this information is limited in the research literature, we did not attempt to include in the model any temporal changes in phosphorus concentrations with treatment. Moreover, even if such changes were implemented, we lacked post-disturbance phosphorus observations at the modeled watersheds to validate model results.

Basin-scale statistical analyses

Management scenario comparison

Analyzing the soil erosion as an average for all the hillslopes and modeled conditions in the basin, we find that, overall, all thinning scenarios narrowly increased sediment and phosphorus yields but not as much as a moderate or high severity fire (Table 9). The annual average hillslope soil erosion from the current conditions was 107 Mg/yr while erosion from thinning varied between 110 Mg/yr for thinning (96%) and 113 Mg/yr for thinning (85%). Conversely the soil erosion for the wildfire scenarios was 298 Mg/yr, 930 Mg/yr, and 6131 Mg/yr for low, moderate, and high severity, respectively (Table 9).

The WEPP model can differentiate between soil detachment and deposition from both hillslopes and channel and can produce outputs by either hillslopes or channels or at the watershed outlets. In this study, we have mainly focused on the results from the hillslopes since they are the main target for forest management activities. However, in addition to the hillslope results, Table 9 also shows the sediment yield, total phosphorus, and sediment yield for particles <16 μm from the watershed outlets. Under current conditions, channels generate more soil erosion than hillslopes, which is expected since undisturbed forests generate minimal sediment yield (Elliot, 2004). With an increase in disturbance, though, despite an increase in sediment yield from hillslopes, total sediment transported to channels will decrease (107 Mg/yr from hillslopes vs 141 Mg/yr from channels for current conditions, compared to 6121 Mg/yr from hillslopes vs 1443 Mg/yr from channels for high severity fire) (Table 9). This shift in erosion between hillslopes and channels with an increase in disturbance is likely due to sediment deposition within the channel network.

The relatively small increase in sediment yield with thinning when compared to current conditions is likely due to the differences in land cover. Our results show that under undisturbed conditions the areas covered by grass and shrub generate substantially more erosion than the areas covered by forests (Fig.

15 in section *Treatment effects on sediment yield for slopes 30–50%*) therefore, the effects of thinning are masked by the grass and shrub areas.

Table 9. Summary of annual average sediment and phosphorus yields from hillslopes and at the watershed outlets.

Condition	Hillslopes Sediment (Mg/yr)	Outlet Sediment (Mg/yr)	Outlet Total P (kg/yr)	Outlet Sediment <16µm (Mg/yr)
Current Conditions	107	141	210	38
Thinning 85%	113	153	227	41
Thinning 93%	111	152	227	41
Thinning 96%	110	152	226	41
Prescribed Fire	183	177	255	46
Low Severity Fire	298	221	310	56
Moderate Severity Fire	930	428	559	103
High Severity Fire	6131	1443	1751	387
SimFire.fccsFuels_obs_cli	285	237	329	59
SimFire.landisFuels fut cli A2	670	474	635	110
SimFire.landisFuels obs cli	278	238	329	59

Estimating Treatment Benefits

Besides directly comparing WEPP model outputs for soil erosion from current conditions to the potential erosion from forest treatments and wildfires, we also calculated the projected change in sediment yield with thinning as an absolute difference between current conditions and thinning at 85%. The treatment benefit estimates were calculated for the Blackwood watershed as an example.

Fig. 12 shows a map of the absolute difference in soil erosion. More yellow or red areas are hillslopes where thinning will generate more erosion than current conditions. A negative value means the hillslope erosion following thinning may be less than erosion for the current condition, likely due to an earlier slower snowmelt following thinning.

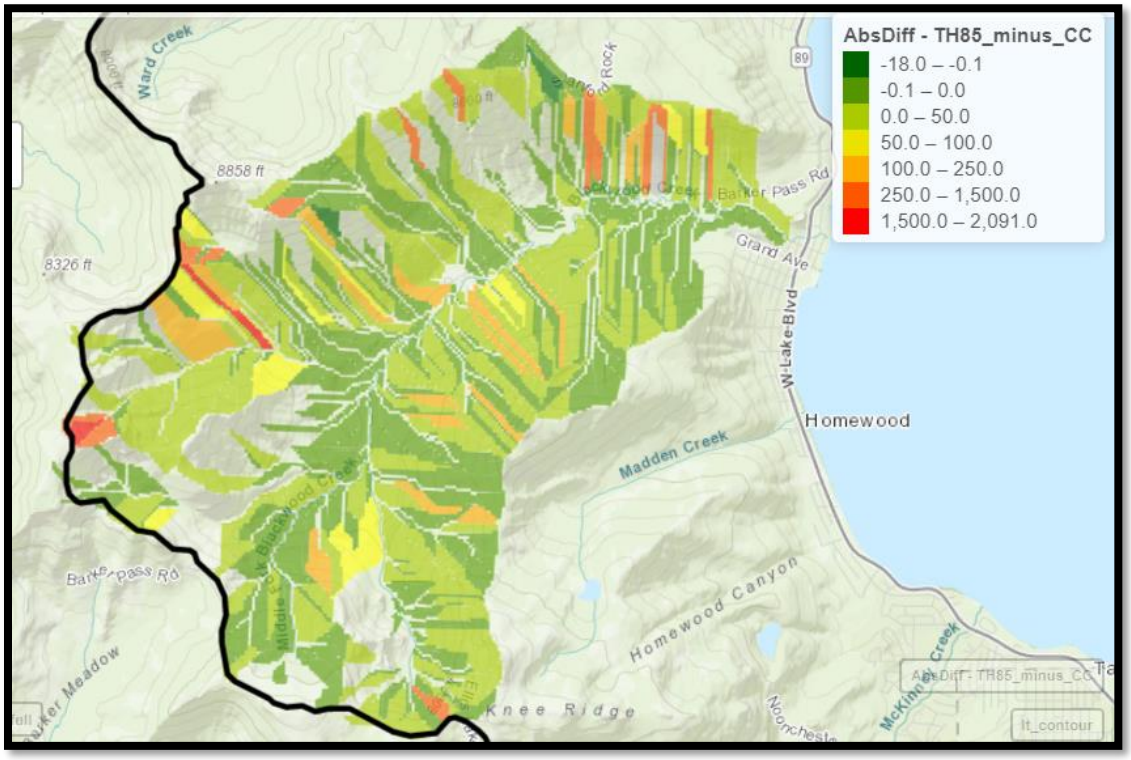

Fig. 12. Absolute sediment yield difference (kg/ha/yr)

Fig. 13 shows the treatment benefit where dark green areas represent greater benefit from thinning. For example, for the most extreme value (treatment benefit: 98,575 kg/ha) soil erosion is predicted as: Current Conditions (1,274 kg/ha), Thinning 85% (3,255 kg/ha), Low Fire (25,074 kg/ha), and Moderate Fire (129,593 kg/ha). Yellow areas are areas where the treatment benefits are non-detectable. The red areas represent hillsopes where current conditions and thinning generate zero erosion while low severity fire generates more erosion than moderate severity. The reason for the moderate severity scenario generating less sediment than low severity is likely due to faster late season snow melt rates predicted for some years beneath the denser low severity canopy compared to the moderate severity canopy. Comparing these results with the results from Fig. 12, it appears that the hillslopes that would erode more after thinning (the redder hillslopes in Fig 12) are also the hillslopes that would benefit more from thinning (greener hillslopes in Fig. 13).

We also calculated treatment benefit from thinning 1, 10, 20, 30, 40, 50, 60 times within the 60 year fire return interval as opposed to only three times. Results show that managers would need to apply thinning treatments more than 50 times within the 60 years, in order to generate erosion that would eliminate the benefits of reducing wildfire severity from moderate to low (Table 10).

Table 10. Average treatment benefit (sediment yield in kg/ha) from increasing thinning within 60 year fire return interval. Results are for the forested hillslopes of Blackwood Creek. Calculation were performed with Eq. 1.

Number of thinning operations	**1**	**3**	**10**	**20**	**30**	**40**	**50**	**60**

Average treatment benefit (kg/ha)	1663	1595	1356	1015	674	333	−8	−349

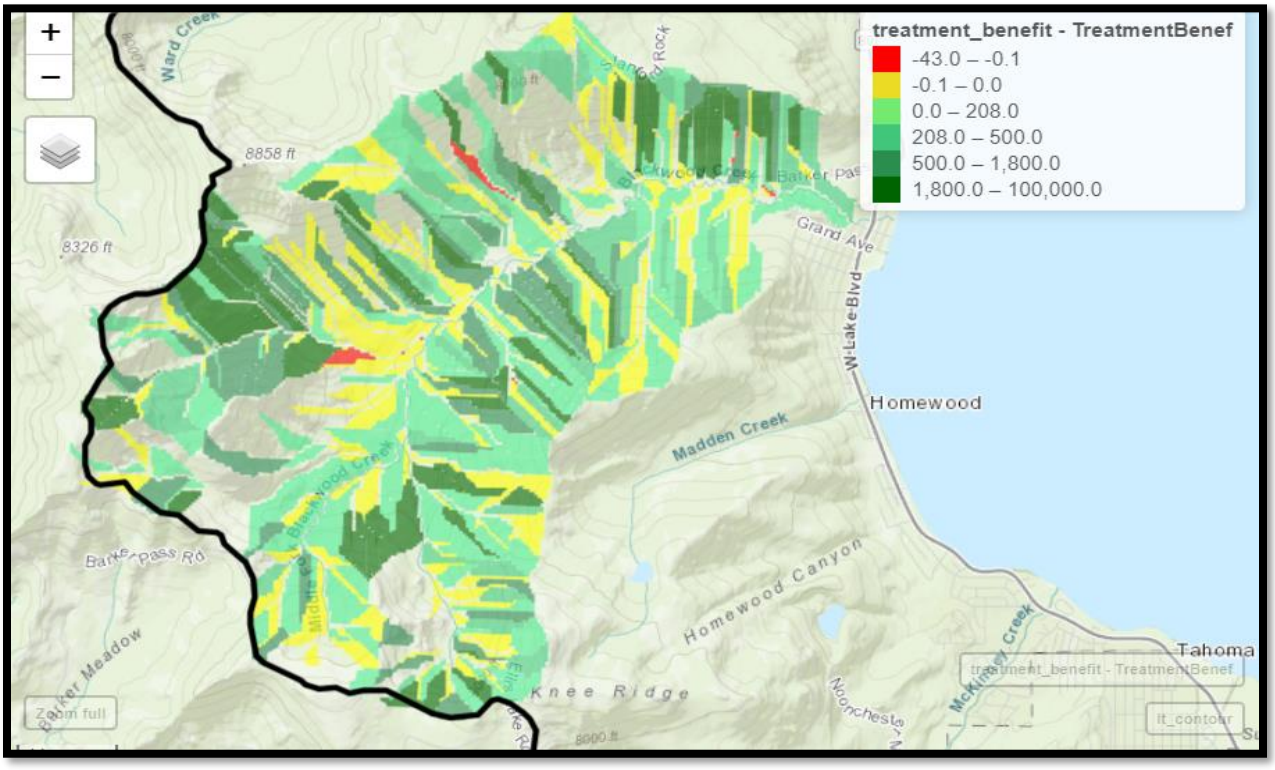

Fig. 13. Example of Treatment Benefit in Blackwood Watershed (kg/ha/yr).

As part of the overall restoration project, treatment polygons have been identified by the stakeholder group for either mechanical thinning on generally flatter slopes and hand or aerial thinning on steeper slopes. Fig. 14 shows the proposed treatment map overlaid on the treatment benefits layer.

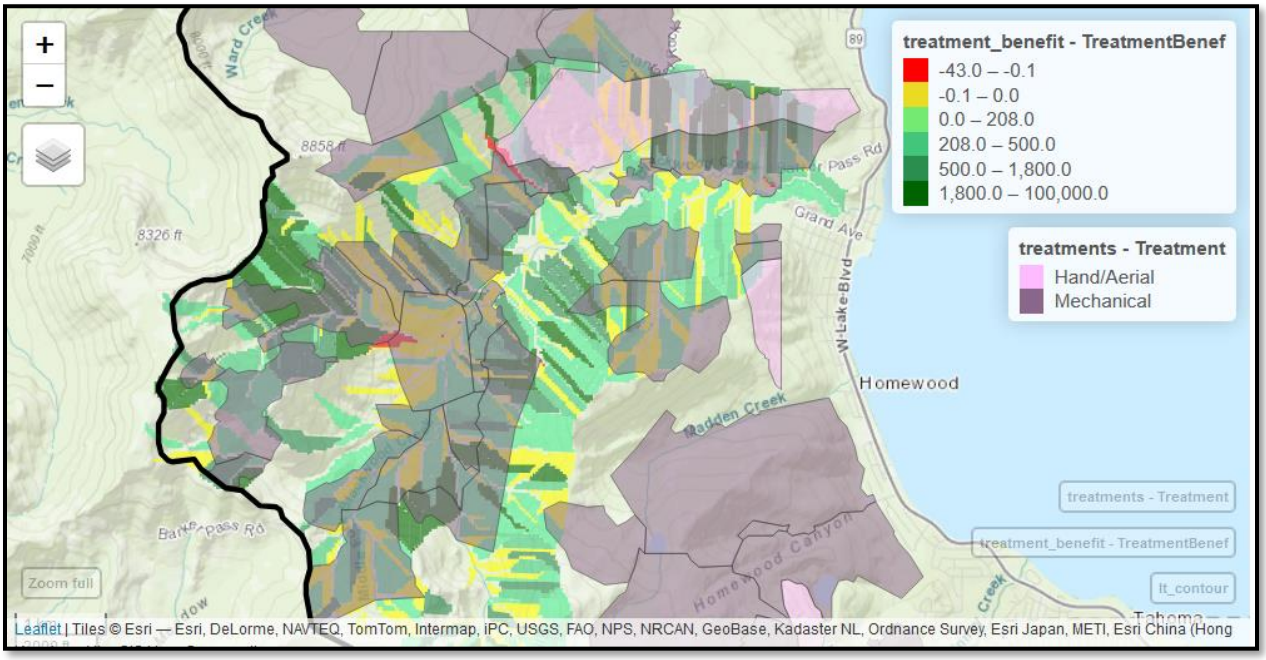

Fig. 14. Treatment benefit overlapped proposed treatment areas (kg/ha/yr).

Treatment effects on sediment yield for slopes 30–50%

We performed several data manipulations and statistical analyses to better understand the effects of slope (specifically those between 30–50%) on sediment yield.

Fig. 15 shows that on gentler slopes (<30%), the bare hillslopes will generate most of the erosion, followed by sod grasses and shrubs. On steeper slopes (>30%), most of the erosion occurred from sod grasses and shrubs. Burn conditions will increase erosion from areas covered by grass and shrubs more than from forests since these areas are generating more erosion than forested areas even under current conditions. We removed from these graphs the three runs based on the SBS predicted maps as those model runs were performed while assuming all hillslopes are forested, and, therefore cannot be compared to the runs where the management scenarios were applied by vegetation type.

Fig. 15. Average sediment yield by vegetation type and slope categories.

Field observations following the Emerald Fire (2016) documented that that two treatment units that had been hand thinned in 2013 experienced low severity wildfire (Kyle Jacobson, Emerald Fire Report). Within those units, which were covered by slopes averaging 30–45%, there were a few areas that experienced high severity fire, which were mainly covered with shrubs. Given that the shrubs areas are generating more erosion than forests, both undisturbed and disturbed conditions, land managers should consider applying treatments on all land covers and not just on forested lands.

Managers are interested expanding thinning treatments to steeper slopes and since thinning will only occur in forested hillslopes, we also analyzed the data by slope steepness only for forested slopes. Results suggest that soil erosion will increase with slope steepness and with increase disturbance (Table 11). Slopes > 30% will generate more erosion than slopes < 30% even in undisturbed conditions (7 kg/ha/yr for slopes 30–50% as compared to 1 kg/ha/yr for slopes <30%). Thinning can increase annual average soil erosion, however less than wildfire. If we only consider the 30−50% hillslopes, thinning (85%) will increase soil erosion by 15 kg/ha/yr (22−7 kg/ha/yr) compared to current conditions. However, since the model results show that wildfire will, on average, increase soil erosion to 4226 kg/ha/yr, it would take 281 years (=4226/15) of annual thinning to reach the sediment yield from one catastrophic wildfire. If we consider the thinning scenario with the least ground disturbance (thinning 96%), it would take 469 (=4226/(16−7)) years of thinning to reach the sediment yield of a high severity wildfire (Table 11). These calculations are purely speculative since it is highly unlikely that a wildfire will burn a watershed uniformly at high severity or that the thinning treatments will be applied on all hillslopes annually, however, they provide a perspective on the difference in erosion between the thinning and the high severity scenarios.

Table 11. Average annual sediment yield (kg/ha) by slope (%) and treatment.

Scenario	<30	30-50	>50
Current Conditions	1	7	10
Thinn 96%	2	16	22
Thinn 93%	2	18	24
Thinn 85%	3	22	30
Prescr_FireF	12	73	98
Low_Severity	22	138	184
Moderate_Severity	142	894	1111
High_Severity	956	4226	5172
SimFire_LANDIS_obsClim	37	207	197
SimFire_FCCS_obsClim	40	207	232
SimFire_LANDIS_futureClim	171	801	887

If we only analyze the data for the undisturbed and 85% thinning conditions, by slope steepness, we find overall low erosion rates from thinning (Table 12). Specifically for the hillslopes between 30–50%, average sediment yield from thinning is 0.14 Mg yr^{-1}. If we further compare the average sediment yield for the 30–50% hillslopes, we find that slope length, specifically slopes >180 m have the potential to generate more erosion from thinning (2.08 Mg yr^{-1}) than slopes < 300 m (0.01 Mg yr^{-1}) (Table 13). We selected these cutoffs to reflect the maximum forest buffer (7−100 m) according to State and Federal guidelines for buffers in the U.S. (Mayer et al., 2005) and the average slope length of the hillslopes within the basin (180 m)

Table 12. Average annual sediment yield by treatment and slope steepness.

Slope steepness (%)	Current Conditions (kg ha^{-1} yr^{-1})	Thinned 85% (kg ha^{-1} yr^{-1})
<30	0.7	2.8
30–50	6.8	21.8
>50	10.4	29.9

Table 13. Average annual sediment yield by treatment and slope length for slopes between 30–50%.

Slope length (m)	Current Conditions (kg ha^{-1} yr^{-1})	Thinned 85% (kg ha^{-1} yr^{-1})
<100	0.004	0.029
100–180	0.068	0.420
>180	15.026	47.735

The odds ratio test between treatment and current conditions indicated that the odds of erosion are higher: 1.71, 1.75, 1.85, 2.59, and 4.4 for Thinn96, Thinn93, Thinn85, Prescribed Fire, and High Severity Fire, respectively. When comparing two treatments, an odds ratio of 1 means that both treatments are equal, while 2 indicates one treatment has twice the odds of occurring as the reference treatment. We found similar results for risk ratio, which calculates the risk of erosion for the entire population of each treatment condition.

The results of the ANOVA analysis were significant (*p-value* < 0.001) suggesting that soil erosion on steeper slopes does increase with treatment, however, the pairwise comparison between each treatment and the current conditions showed that only prescribed fire and high severity fires were significant and not thinning. This suggests that even the most extreme thinning technique will not greatly affect the overall soil erosion in the basin.

From both the ANOVA and the odds ratio analyses we can conclude that thinning will increase the risk of erosion, but when thinned hillslopes erode, the sediment yield is no different from an untreated hillslope (roughly 8 kg ha^{-1}).

Variable importance

The next analyses are based on a series of variables created from the model input files. These include sediment yield (kg $ha^{-1}yr^{-1}$), and various variables related to hillslope physical attributes, topography, and soils (Table 14).

Correlations

Results for all variables and watersheds suggest that for current condition model results sediment yield is positively correlated with hillslope length (*p-value* = 0.39), precipitation (*p-value* = 0.23), hillslope area (*p-value* = 0.22), and percent slope (*p-value* = 0.19) (Table 15). These results suggest that soil erosion increases on longer and larger hillslopes and on those that receive more precipitation. For the disturbed conditions, we found similar correlations, however, they increase with condition in the following order: thinning, prescribed fire, high severity fire (Table 15). Some variables were negatively correlated with sediment yield: plant available water (*p-value* = −0.20), slope width (*p-value* = −0.20), and total soil saturation amount (*p-value* = −0.21). While these correlations are not strong, they suggest that soil erosion increases with a decrease in soil moisture. The negative correlation with slope width implies that soil erosion is greater on narrower slopes. This is perhaps because narrower slopes tend to also be found on steeper slopes at high elevation, and therefore have a greater risk of erosion.

Table 14. List of variables used in the variable importance data analyses.

Variable	Description
Sediment_kg_ha	Sediment Yield in (kg/ha)
precip_mm	Precipitation (mm)
length_m	Slope Length (m)

width	Slope Width (m)
area_ha	Area (ha)
aspect	Aspect (degrees)
slope	Slope (%)
TEXT	Texture (Volcanic/Granitic/Alluvial)
LNDUS	Landuse
albedo	Albedo (0-1)
ani	Anisotropy (-)
bd	Bulk Density (kg/m3)
bed_ksat	Hydraulic conductivity of the underlying geology (mm/hr)
kinter	Interrill erodibility (kg s/m-4)
cec	Cation Exchange Capacity (meq/100g)
clay	Clay (%)
fc	Field Capacity (m3/m3)
fc_rc	Field Capacity corrected for rock content (m3/m3)
horizons	No of soil horizons
krill	Rill erodibility (s/m)
ksat	Saturated hydraulic condictivity (mm/hr)
mukey	Soil name/key from SSURGO
om	Organic matter (%)
plant_available_water_mm	Plant available water (mm)
rocks	Rocks (%)
sand	Sand (%)
sat_wat_conc_rc	Saturated water content (m3/m3)
tauc	Critical Shear (Pa)
total_depth	Total soil depth (mm)
total_sat_amt_mm	Total saturation ammount (mm)
wp	Wilting Point (m3/m3)
wp_rc	Wilting point corrected for rock content (m3/m3)
Elev	Elevation (m)

Table 15. Spearman correlations (*p-values*) of sediment yield with all variables based on the model results from all watersheds. See Table 14 for variable names.

Variables	Current Conditions	Thinning 85%	Prescribed Fire	High Severity Fire
length_m	0.39	0.48	0.51	0.59
precip_mm	0.23	0.32	0.33	0.41
area_ha	0.22	0.28	0.32	0.40
slope	0.19	0.21	0.22	0.18
anis	0.18	0.22	0.13	0.11
Elev	0.13	0.17	0.14	0.17
ksat	0.12	0.13	0.03	−0.03
bd	0.10	0.09	−0.02	−0.07
rocks	0.08	0.09	0.18	0.23
wp	0.06	0.11	0.16	0.23
om	0.05	0.09	0.09	0.12
clay	0.05	0.07	0.16	0.25
cec	0.03	0.06	0.16	0.26
sand	0.02	0.00	−0.10	−0.20
wp_rc	−0.01	0.00	−0.01	−0.01
aspect	−0.03	−0.04	−0.07	−0.10
albedo	−0.05	−0.07	−0.04	−0.02
fc	−0.08	−0.05	−0.01	0.02
fc_rc	−0.10	−0.10	−0.14	−0.16
sat_wat_conc_rc	−0.13	−0.15	−0.20	−0.23
bed_ksat	−0.14	−0.19	−0.16	−0.23
total_depth	−0.15	−0.19	−0.12	−0.12
horizons	−0.16	−0.18	−0.08	−0.02
plant_available_water_mm	−0.20	−0.23	−0.21	−0.24
width	−0.20	−0.23	−0.20	−0.20
total_sat_amt_mm	−0.21	−0.25	−0.22	−0.26

When considering the data by individual watersheds, the correlations between sediment yield and slope length are much stronger for Blackwood, Ward, and Upper Truckee Watersheds (e.g. for Blackwood the *p-value* = 0.64, 0.79, 0.80, and 0.88 for Current Conditions, Thinning, Prescribed Fire, and High Severity fire, respectively). Interestingly, the correlations with precipitation were much weaker when considering the data by watershed, which suggests that precipitation is more important regionally (west/east) rather than locally (within watershed). Slope area, percent slope, and elevation were also strongly correlated with sediment yield for all watersheds, however, for Trout, bulk density (*p-value* = 0.35), and anisotropy (*p-value* = 0.35), were slightly more correlated with sediment yield than slope length (*p-value* = 0.31) (Tables 16−19).

The positive correlation between sediment yield and hillslope area could be indirectly because of the correlation between slope length and hillslope area *(p-value* = 0.71; data not shown). Similarly, sediment yield increases with elevation, which could also be because slope steepness increases with elevation (*p-value* = 0.38; data not shown) and also because higher elevation areas, especially in watersheds like Blackwood and Ward, are characterized by sparser vegetation and rock outcrops, which generate more erosion.

Soil bulk density is calculated as the dry weight of soil divided by its volume and it increases with compaction and depth. Our results show that soil erosion increases with bulk density for the Trout watershed (Table 18). This is likely due to the fact that soils with high bulk densities also tend to have

more sands, less organic matter, and less available water capacity. Soil anisotropy is a term used to denote preferential flow direction in soils and depends on the structure of the soil. Soil anisotropy ratio signifies a prevalence of lateral versus vertical hydraulic conductivity. In soils with higher anisotropy values, water movement through the soil profile is higher laterally than vertically, and is higher in steeper slopes (Zaslavsky and Rogowski, 1969). In WEPP, a value of 10 (unitless) is assigned for the first 400 mm of soil depth and 1 (unitless) for the remaining soil depth. The positive correlation between anisotropy and erosion suggests that soil erosion increases on slopes with greater lateral flow, and therefore on steeper slopes.

Table 16. Spearman correlations (*p-values*) of sediment yield with all variables based on the model results for the Blackwood Creek watershed. See Table 14 for variable names.

Variables	Current Conditions	Thinning 85%	Prescribed Fire	High Severity Fire
length_m	0.64	0.79	0.80	0.88
area_ha	0.43	0.54	0.60	0.69
slope	0.29	0.37	0.39	0.39
Elev	0.23	0.25	0.25	0.33
albedo	0.15	0.11	0.10	0.08
anis	0.15	0.13	0.12	0.13
wp	0.13	0.13	0.16	0.09
precip_mm	0.07	0.05	0.07	0.12
bd	0.06	0.08	0.09	0.03
clay	0.05	0.05	0.05	0.02
fc	0.04	0.04	0.10	0.02
rocks	0.03	0.00	−0.05	0.05
cec	0.02	0.00	−0.04	0.06
wp_rc	0.01	0.03	0.07	−0.02
om	0.00	0.00	−0.02	0.04
horizons	−0.02	−0.03	−0.01	−0.01
ksat	−0.02	−0.01	−0.07	0.01
fc_rc	−0.02	−0.01	0.04	−0.05
aspect	−0.05	0.04	0.07	0.06
sand	−0.06	−0.04	0.01	−0.06
plant_available_water_mm	−0.07	−0.05	−0.01	−0.09
total_sat_amt_mm	−0.08	−0.07	−0.02	−0.11
total_depth	−0.08	−0.07	−0.03	−0.12
sat_wat_conc_rc	−0.08	−0.06	−0.01	−0.09
bed_ksat	−0.18	−0.13	−0.13	−0.13
width	−0.31	−0.34	−0.28	−0.27

Table 17. Spearman correlations (*p-values*) of sediment yield with all variables based on the model results for the Ward Creek watershed. See Table 14 for variable names.

Variables	Current Conditions	Thinning 85%	Prescribed Fire	High Severity Fire
length_m	0.60	0.73	0.76	0.86
area_ha	0.37	0.50	0.53	0.67
slope	0.25	0.35	0.40	0.44
Elev	0.22	0.24	0.19	0.33
albedo	0.17	0.22	0.27	0.25
clay	0.17	0.09	0.05	−0.04
anis	0.16	0.20	0.24	0.22
precip_mm	0.14	0.11	0.06	0.11
rocks	0.13	0.18	0.18	0.24
ksat	0.11	0.12	0.09	0.11
bd	0.10	0.00	−0.05	−0.16
cec	0.10	0.18	0.17	0.27
wp	0.06	0.00	−0.01	−0.12
aspect	−0.02	−0.02	−0.01	0.02
om	−0.09	0.00	0.02	0.11
wp_rc	−0.09	−0.14	−0.15	−0.22
sand	−0.12	−0.07	0.00	−0.01
fc	−0.12	−0.15	−0.13	−0.20
fc_rc	−0.13	−0.18	−0.17	−0.23
plant_available_water_mm	−0.16	−0.20	−0.20	−0.23
total_depth	−0.20	−0.24	−0.23	−0.26
total_sat_amt_mm	−0.20	−0.24	−0.23	−0.27
horizons	−0.21	−0.10	−0.04	0.04
sat_wat_conc_rc	−0.21	−0.25	−0.24	−0.27
bed_ksat	−0.25	−0.22	−0.19	−0.13
width	−0.34	−0.33	−0.33	−0.27

Table 18. Spearman correlations (*p-values*) of sediment yield with all variables based on the model results for the Trout Creek watershed. See Table 14 for variable names.

Variables	Current Conditions	Thinning 85%	Prescribed Fire	High Severity Fire
bd	0.35	0.41	0.41	0.43
anis	0.35	0.38	0.38	0.36
length_m	0.31	0.40	0.41	0.53
sand	0.30	0.30	0.28	0.20
Elev	0.26	0.32	0.31	0.40
slope	0.24	0.29	0.29	0.33
wp	0.21	0.19	0.21	0.17
wp_rc	0.20	0.17	0.17	0.09
area_ha	0.19	0.22	0.24	0.31
precip_mm	0.16	0.21	0.21	0.21
ksat	0.06	0.09	0.08	0.14
rocks	0.00	0.05	0.05	0.14
clay	−0.01	0.01	0.02	0.08
cec	−0.01	0.02	0.02	0.09
fc_rc	−0.03	−0.08	−0.08	−0.17
aspect	−0.04	−0.05	−0.06	−0.03
om	−0.06	−0.09	−0.09	−0.09
width	−0.14	−0.19	−0.19	−0.25
sat_wat_conc_rc	−0.14	−0.20	−0.20	−0.29
fc	−0.17	−0.20	−0.18	−0.20
bed_ksat	−0.17	−0.19	−0.20	−0.22
albedo	−0.28	−0.27	−0.26	−0.19
horizons	−0.32	−0.32	−0.32	−0.28
plant_available_water_mm	−0.32	−0.37	−0.36	−0.39
total_sat_amt_mm	−0.34	−0.40	−0.39	−0.43
total_depth	−0.35	−0.37	−0.37	−0.37

Table 19. Spearman correlations (*p-values*) of sediment yield with all variables based on the model results for the Upper Truckee Watershed. See Table 14 for variable names.

Variables	Current Conditions	Thinning 85%	Prescribed Fire	High Severity Fire
length_m	0.54	0.66	0.67	0.73
area_ha	0.36	0.47	0.49	0.55
slope	0.32	0.35	0.37	0.32
Elev	0.21	0.29	0.29	0.33
bd	0.10	0.08	0.06	0.07
anis	0.08	0.15	0.15	0.17
clay	0.08	0.06	0.06	0.07
rocks	0.07	0.05	0.04	0.02
precip_mm	0.07	0.16	0.18	0.22
ksat	0.06	0.04	0.03	0.00
wp	0.04	0.07	0.09	0.14
cec	0.03	0.03	0.03	0.04
wp_rc	−0.02	0.01	0.03	0.07
albedo	−0.02	−0.06	−0.07	−0.11
fc	−0.03	0.00	0.02	0.07
bed_ksat	−0.03	−0.06	−0.07	−0.08
sand	−0.04	−0.02	−0.02	−0.03
aspect	−0.04	−0.05	−0.05	−0.05
om	−0.07	−0.03	−0.02	0.00
total_depth	−0.07	−0.13	−0.13	−0.17
fc_rc	−0.08	−0.05	−0.03	0.01
horizons	−0.09	−0.13	−0.14	−0.15
plant_available_water_mm	−0.09	−0.12	−0.12	−0.12
total_sat_amt_mm	−0.12	−0.16	−0.16	−0.18
sat_wat_conc_rc	−0.12	−0.11	−0.10	−0.08
width	−0.25	−0.25	−0.24	−0.22

PCA

The PCA analysis revealed similar relationships between variables for all management condition. For comparison we are only presenting the results for current conditions and high severity fire (Figs. 16 and 17). The first two components of PCA, cumulatively, explained 41% of variance for all management conditions. The data seems to be spread uniformly along the two principal components, however, data groups in small clusters, which is likely due to differences among individual watersheds. Additionally, higher sediment yield values are mainly found on the negative values for component 1 and positive values for component 2, while lower sediment yield values are mainly found on the positive values for component 1 and negative values for component 2. This pattern is more apparent for the results based on the high severity management scenario. While the loading of the sediment yield variable does not have a significant weight on the two principal components compared to other variables, it is in the same direction as slope length, slope area, slope width, % rocks, % organic matter,

precipitation, and albedo, which signifies positive correlations with these variables. From the PCA analysis we cannot draw clear conclusions regarding sediment yield and slope, however, the analysis helps us better understand the relationships between the data.

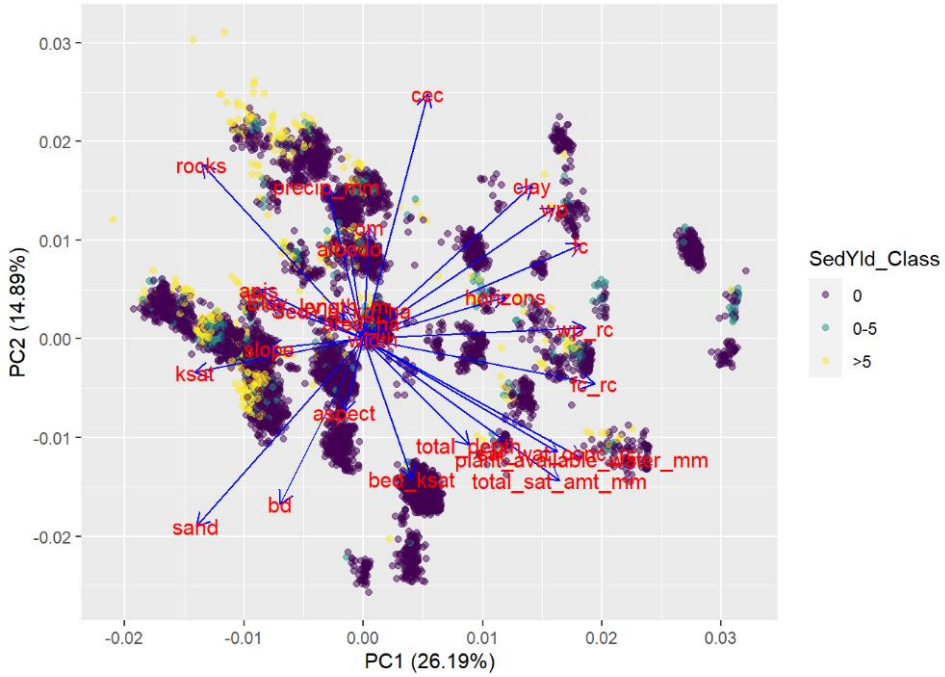

Fig. 16. Results of the principle component analysis for the 27 environmental variables based on all forested hillslope for current conditions. The colors represent sediment yield classes. Description of variable abbreviations can be found in Table 14.

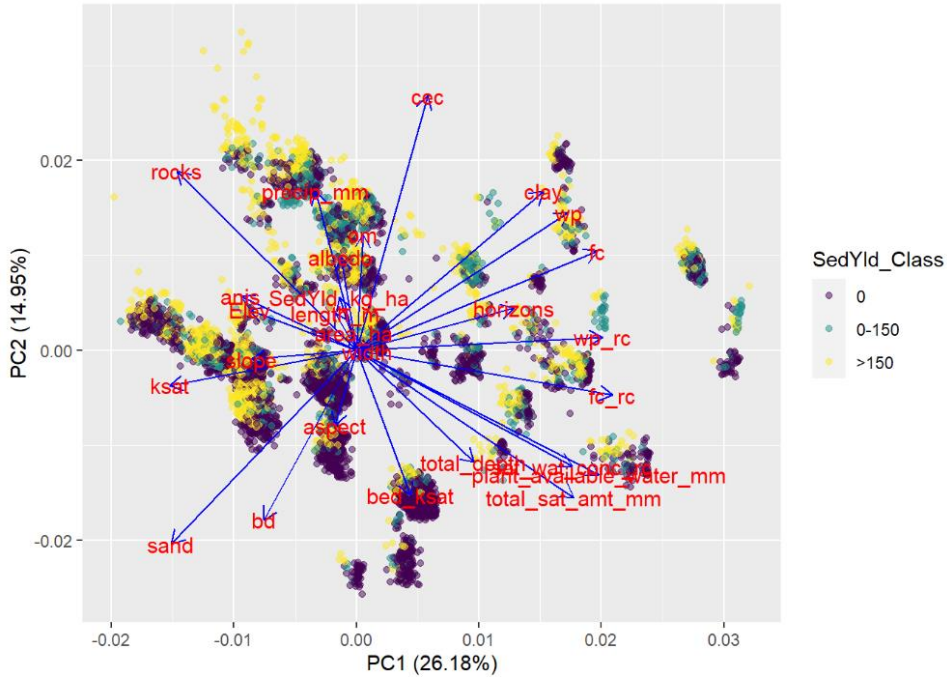

Fig. 17. Results of the principle component analysis for the 27 environmental variables based on all forested hillslope for high severity fire. The colors represent sediment yield classes. Description of variable abbreviations can be found in Table 14.

RF

We first applied the random forest model to predict weather a hillsope will erode or not. Under current conditions, approximately 10% of the hillslopes across the Lake Tahoe Basin erode, while under high severity fire, the percentage increases to slightly over 40% (Fig. 18, left column). These results suggest, at least according to the WEPP model, that approximately 60% of the hillslopes will not erode even under high severity fire, which is the most extreme modeled scenario. The non-eroding hillslopes are mainly found in the eastern-side of Lake Tahoe (Fig. 11), however, all watersheds, including the highly eroding ones such as Blackwood and Upper Truckee also have non-eroding hillslopes.

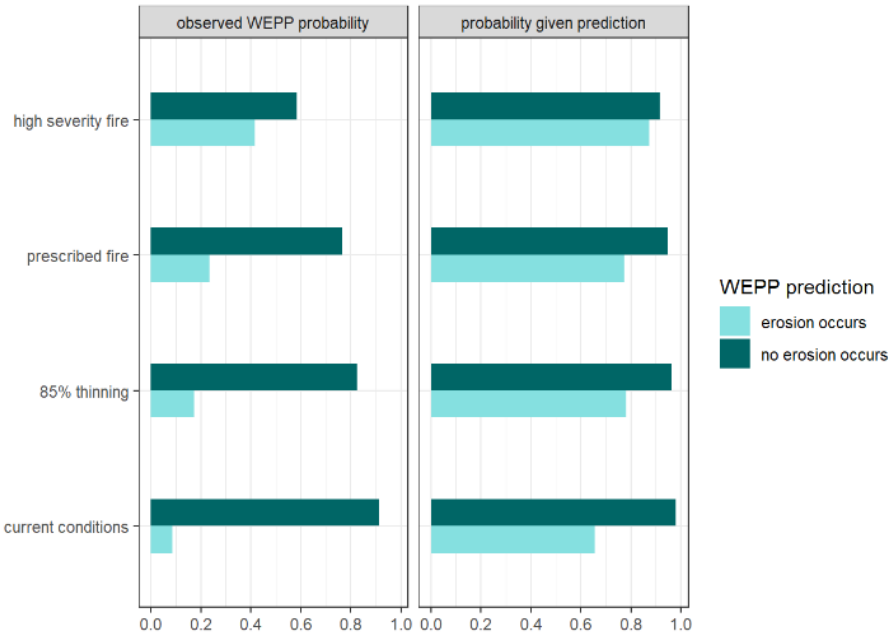

Fig. 18. Accuracy of the random forest prediction of eroding vs. non-eroding hillslopes by management scenario.

To better understand the differences between the hillslopes that erode and those that do not erode, we calculated the average values for several environmental variables by hillslopes that erode and those that do not erode. Table 20 shows that hillslopes that do not erode, have on average shorter hillslopes lengths, receive less precipitation, have smaller areas and wider widths, and are mainly facing SSW slopes. Both elevation and slope were similar for hillslopes from the two erosion categories.

Table 20. Averages of sediment yield and environmental variables by hilllsopes that erode vs. those that do not erode.

SedVar	Sediment Yield (kg/ha)	Slope Length (m)	Slope Steepness (%)	Precipitation (mm)	Elevation (m)	Area (ha)	Width (m)	Aspect (degrees)	Soil Depth (mm)
NoErod	0	114	0.24	917	2228	3.63	349	206	1223
Erod	5190	272	0.27	1119	2281	6.06	298	180	1152

Plotting the variable importance from the random forest model, we find that the most important variables for predicting areas that erode are: slope length, followed by precipitation, %slope, slope area, slope width, and elevation (Fig. 19). While slope length and precipitation are at the top for each of the four management scenarios compared in this analysis, the order of the other variables varies with scenario (Fig. 19).

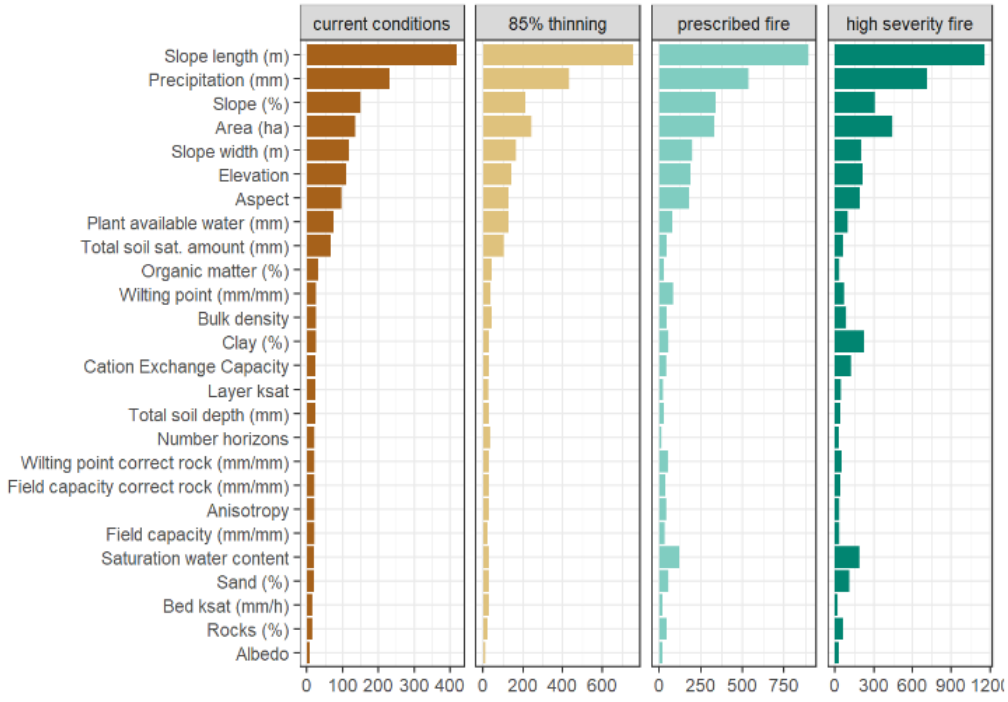

Fig. 19. Variable importance for the RF model (testing eroding vs. non-eroding hillslopes) by management scenario.

We then applied the RF model to predict actual values of sediment yield. The RF model accurately predicted soil erosion for all four management conditions (Fig. 20). Plotting the % increase in Mean Squared Error (MSE) we find that, similar to the previous analysis, the most important variables for predicting sediment yield are length, followed by %slope and precipitation (Fig. 21).

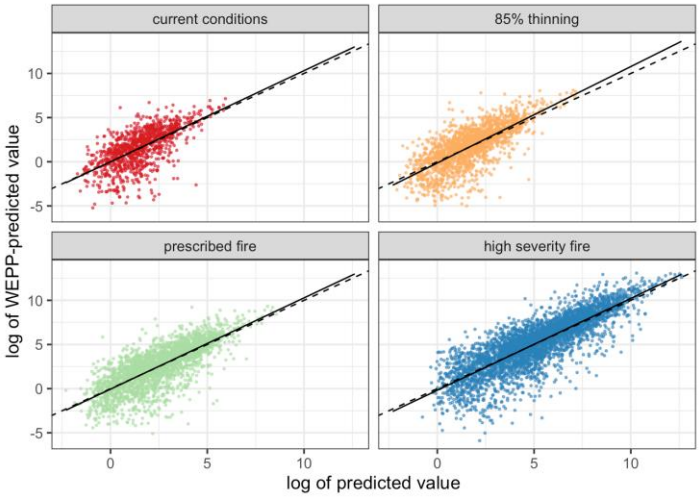

Fig. 20. WEPP-predicted vs RF predicted sediment yield based on several environmental variables.

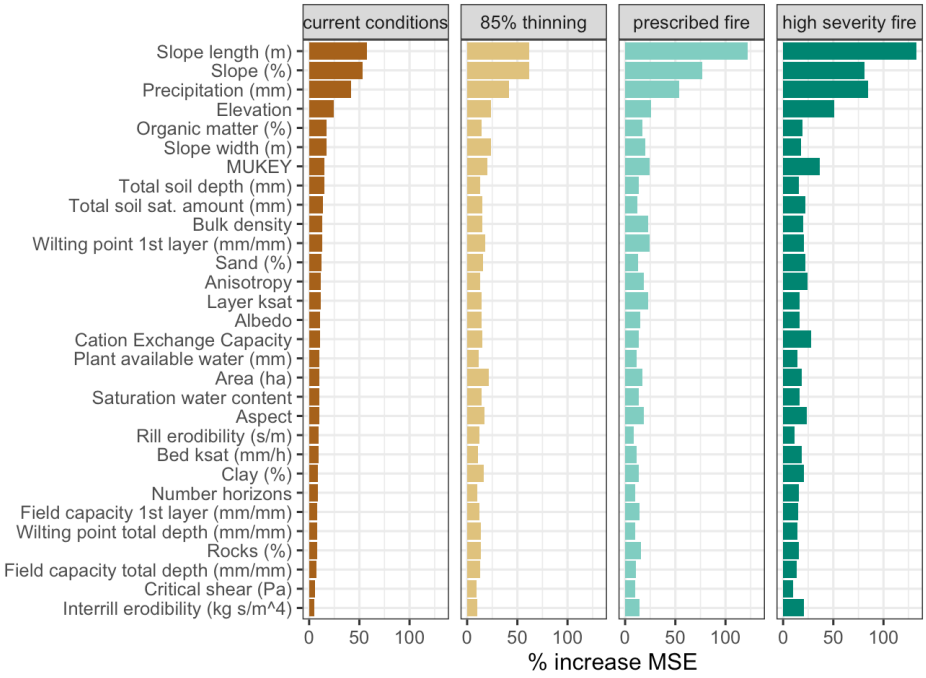

Fig. 21. Percent increase in mean squared error (MSE) by modeled variables and scenarios.

Additional graphs and data summaries

Fig. 22 shows the top ten watersheds within the Lake Tahoe Basin with the greatest sediment delivery from hillslopes for the undisturbed conditions. These calculations are performed by selecting only the forested hillslopes.

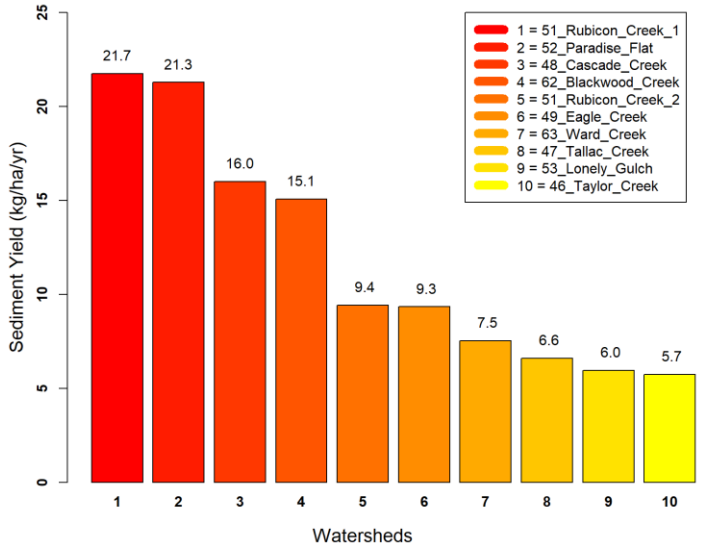

Fig. 22. Ten watersheds with the greatest sediment delivery from hillslopes to channels for the undisturbed forest conditions.

The order of the watersheds changes when accounting for the watershed area (Fig. 23). Blackwood, Upper Truckee, and Ward are the greatest contributors.

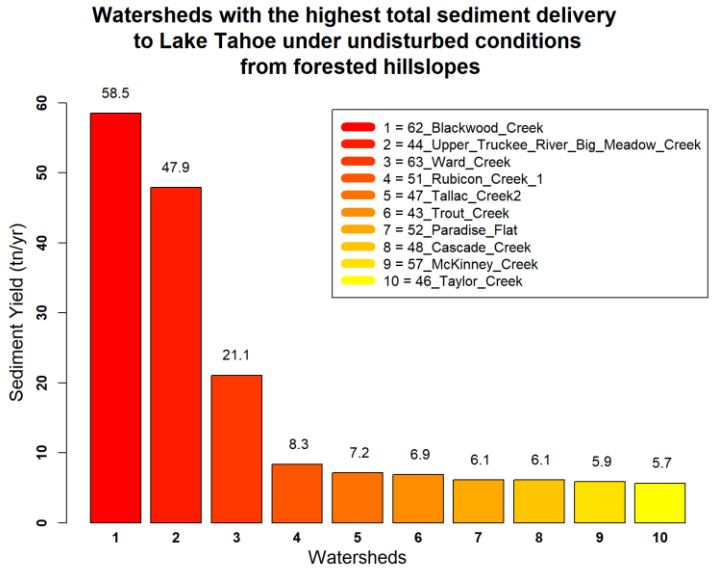

Fig. 23. Top ten watersheds delivering sediment to Lake Tahoe.

Soil erosion and sediment delivery are influenced by topography, land cover, soil properties and climate. Based on the hillslope output data we created additional tables to quantify the effects of each

of these individual factors on soil erosion. All calculations are based on the model results from the current condition scenario. Variable precipitation, was split based on the average precipitation at all the hillslopes within the basin (1000 mm). Tables 20−24 show the average sediment yield by various variables. From these tables we can conclude:

- Volcanic soils erode more than granitic and alluvial soils (Table 21);
- Sediment yield is greatest on hillslope that receive more than 1000 mm of precipitation and have slopes > 50%; The least sediment yield is found on hillslopes with less than 1000 mm precipitation and slope steepness < 30% (Table 22);
- Hillslopes between 2600−2800 m generate more erosion than hillslopes found at both lower and higher elevation (Table 23);
- Soil erosion is greater on soils with more rock outcrops (e.g. Melody and Ellispeak) (Table 24);
- Soil erosion is similar on all aspects, except on western slopes, where soil loss is less than half of the soil loss predicted on south-, north-, and east-facing slopes (Table 25).

Table 21. Average sediment yield (kg/ha) by texture and condition.

Texture	Current Conditions	Thinning 85%	Prescribed Fire	High Severity Fire
Alluvial	1.64	4.05	22	519
Granitic	2.22	5.48	21	1278
Volcanic	6.03	23.42	77	5431

Table 22. Average sediment yield by slope steepness and precipitation.

Precipitation Category	Slope Steepness	Sediment yield (kg/ha)	Sediment yield (tonnes)
<1000mm	<30	0.08	0.0005
>1000mm	<30	1.38	0.0087
<1000mm	>50	3.31	0.0272
>1000mm	>50	16.93	0.1157
<1000mm	30−50	0.63	0.0045
>1000mm	30−50	13.70	0.0911

Table 23. Average soil loss by elevation (m).

Elevation Category	Sediment yield (kg/ha)	Sediment yield (tonnes)
<1800	0.0	0.00
1800−2000	0.36	0.00

2000−2200	1.70	0.01
2200−2400	3.26	0.02
2400−2600	5.33	0.03
2600−2800	8.98	0.05
2800−3000	3.89	0.03
>3000	0.05	0.00

Table 24. Average soil loss by top ten eroding soils.

Soil Name	Sediment yield (kg/ha)
Melody-Rock outcrop complex	83
Lithnip-Meiss-Hawkinspeak association	59
Ellispeak-Rock outcrop complex	44
Rubble land-Glenalpine complex	33
Meeks extremely stony loamy coarse sand	26
Ellispeak-Waca complex	21
Waterpeak-Rock outcrop complex	19
Temo-Witefels complex	16
Tinker-Rock outcrop	11
Mountrose-Wardcreek-Melody complex	10

Table 25. Average soil loss by aspect.

Aspect	Sediment yield (kg/ha)	Sediment yield (tonnes)
E	3.99	0.02
N	3.75	0.02
S	3.93	0.03
W	1.45	0.01

V. CONCLUSIONS

In the current study, we demonstrated that the WEPPcloud interface can successfully simulate general trends in streamflow, sediment, and phosphorus in watersheds with different physiographic settings with minimal calibration. Additionally, we demonstrated the applicability of the interface to various forest fuel treatments and wildfire scenarios, which can provide land and water resources managers with site-specific information of the spot areas in their watersheds to control soil erosion and phosphorus transport with forest management practices. The minimal calibration performed in this study involved manual alterations of calibrating parameters that are not easily found in national databases (i.e., kb, Ksub, τc, P concentrations). However, previous research, and the current study,

demonstrate that at least some of these parameters could be inferred from geology (kb) or could be determined from observed data at nearby watersheds (kb, τc, P concentrations).

The results from the treatment benefit calculations for Blackwood, revealed the sensitive areas within the watershed that are more prone to erosion. The results suggest that hillslopes that are more prone to erosion post-thinning would also benefit more from thinning by avoiding high erosion rates from a potential wildfire.

Land managers were interested to determine if thinning would increase sediment yield on steeper slopes (30−50%). To address this question we performed several data summaries and statistical analyses, which showed that when we analyze the data considering all vegetation types, most sediment yield on slopes between 30−50% comes from areas covered by shrubs and grasses and not from forested areas, which suggests that land managers should consider applying treatments on all land covers and not just on forested lands.

The results from the ANOVA and the odds ratio analyses on hillslopes between 30 and 50% showed that thinning will increase the risk of erosion, but when thinned hillslopes erode, the sediment yield is no different when compared to an untreated hillslope. When we further plotted the data by slope length we found that longer hillslopes generate significantly more sediment yield than shorter slopes. Additional data analyses revealed other variables that are influencing soil erosion in the basin, however, slope length was consistently identified as a major driver. Therefore managers should consider thinning activities that either include buffers or add natural breaks along the slopes (i.e. thin only portions of a slope).

Mechanical thinning has the potential to generate more erosion through soil disturbances related to rutting, however, current management practices are likely to address this risk by using slash mats (harvest residue on which harvesting machinery can move) or other methods to minimize soil disturbance and increase ground cover. Newer mechanized equipment (with flexible tracks or frames, or with tethering), which were designed to be operated on steep terrains, can further minimize soil disturbance. Similarly, newer harvesting machines are equipped with larger inflatable wheels and they can also carry instead of dragging logs from site-to-site, which reduce compaction and minimize disturbance.

This modeling study showed that thinning minimally increased soil erosion when compared to the results from the wildfire. A large body of research suggests that forest treatments will help decrease risks of wildfire, with important social benefits.

Other mitigation strategies to minimize impacts of treatments on sediment and water quality include:

- Encouraging high patchiness of treatments.
- Staggering treatments in time and space to minimize cumulative impacts at the watershed outlet.
- Designing topographically-based buffers to reduce the connectivity of potential source areas to stream networks. These buffers could be strips of undisturbed soils on long slopes and at the bottom of steep slopes. This approach would be distinct from standard stream zone buffers, as full restoration goals may include thinning and burning within riparian areas.

- Planning upland treatments to follow meadow restoration projects that are designed to help capture eroded sediments and burned debris on floodplains. Such effects have been suggested for meadow restoration projects to mitigate channel incision, such as at Trout Creek.
- Using care when reopening roads to access areas for thinning to minimize erosion risk.

REFERENCES

Abatzoglou J.T., Lasslop G. and Bachelet D. (2020) Editorial: Climate, Land Use, and Fire: Can Models Inform Management? *Front. Earth Sci.* 8:624171. doi: 10.3389/feart.2020.624171.

Agee, J.K., and Skinner, C.N. (2005) Basic principles of fuel reduction treatments. Forest Ecology and Management 211:83–96.

Beck, H.E., van Dijk, A.I.J.M., Miralles, D.G., de Jeu, R.A.M., Bruijnzeel, L.A., McVicar, T.R., Schellekens, J. (2013) Global patterns in base flow index and recession based on streamflow observations from 3394 catchments. *Water Resour. Res*. 49, 7843–7863.

Benavides-Solorio, J.D., MacDonald, L.H. (2005) Measurement and prediction of post-fire erosion at the hillslope scale, Colorado Front Range. *Int. J.Wild. Fire*. 14, 457–474. doi:10.1071/WF05042.

Berenbrock, C., Tranmer, W.A. (2008) Simulation of flow, sediment transport, and sediment mobility of the lower Coeur d'Alene river, Idaho, USGS Scientific Investigation Report, pp 43.

Bowman, D.M., Kolden, C. A., Abatzoglou, J.T., Johnston, F.H., van der Werf, G.R., and Flannigan, M. (2020) Vegetation fires in the anthropocene. *Nat. Rev. Earth Environ.* 1 (10), 500–515. doi:10.1038/s43017-020-0085-3.

Brooks, E.S., Dobre, M., Elliot, W.J., Wu, J.Q., Boll, J. (2016) Watershed-scale evaluation of the Water Erosion Prediction Project (WEPP) model in the Lake Tahoe basin. *J. Hydrol*. 533, 389–402. doi:10.1016/j.jhydrol.2015.12.004.

Busse, M.D., Shestak, C., Gerard, R. (2018) Pile burning in the Lake Tahoe Basin: field observations nine years after burning. Davis, CA: USDA Forest Service Pacific Southwest Research Station. 15 p.

Christensen, W., Norman, S. (2007) Ward Unit 5 Soil Monitoring Report. South Lake Tahoe, CA: USDA Forest Service Lake Tahoe Basin Management Unit. 26 p. https://www.fs.usda.gov/Internet/FSE_DOCUMENTS/fsm9_045980.pdf

Coats, R., Costa-Cabral, M., Riverson, J., Reuter, J., Sahoo, G., Schladow, G., Wolfe, B. (2013) Projected 21st century trends in hydroclimatology of the Tahoe basin. *Clim. Change* 116:51–69.

Coats, R., Lewis, J., Alvarez, N., Arneson, P. (2016) Temporal and spatial trends in nutrient and sediment loading to Lake Tahoe, California-Nevada, USA. *J. Am. Water Resour. Assoc*. 52, 1347–1365. doi:10.1111/1752-1688.12461.

Coop, J.D., S.A., Parks, C.S., Stevens-Rumann, S.D., Crausbay, Higuera, P.E., Hurteau, M.D. (2020) Wildfire-driven forest conversion in western north American landscapes, *Bioscience* 70 (8), 659–673. doi:10.1093/biosci/biaa061.

Cram, D.S., Baker, T.T., Fernald, A.G., Madrid, A., Rummer, B. (2007) Mechanical thinning impacts on runoff, infiltration, and sediment yield following fuel reduction treatments in a southwestern dry mixed conifer forest. *J. Soil Water Cons.* 62(5): 359–366.

Deval, C., Brooks, E.S., Gravelle, J.A., Link, T.E., Dobre, M., Elliot, W.J. (2021) Long-term response in nutrient load from commercial forest management operations in a mountainous watershed. *For. Ecol. Manage*. 494, 119312. doi:10.1016/j.foreco.2021.119312.

Elliot, W.J. 2004. WEPP internet interfaces for forest erosion prediction. *J. Am. Water Res. Ass.* 40(2):299–309. https://doi.org/10.1111/j.1752-1688.2004.tb01030.x.

Flanagan, D.C., Nearing, M.A. (1995) Water Erosion Prediction Project hillslope profile and watershed model documentation. NSERL Report #10, USDA-ARS National Soil Erosion Research Laboratory, West Lafayette, IN.

Flanagan, D.C., Gilley, J.E., Franti, T.G. (2007) Water Erosion Prediction Project (WEPP): development, model capabilities, and future enhancements. *Trans. ASABE*. 50(5), 1603–1612.

Fox, D.M., Bryan, R.B. (2000) The relationship of soil loss by interrill erosion to slope gradient. *Catena*. 38(3): 211–222.

Gao, X., Chen, N., Yu, D., Wu, Y., Huang, B. (2018) Hydrological controls on nitrogen (ammonium versus nitrate) fluxes from river to coast in a subtropical region: Observation and modeling. *J. Environ. Manage*. 213, 382‑391. doi:10.1016/j.jenvman.2018.02.051.

Garbrecht, J., Martz, L.W. (1997) TOPAZ: An automated digital landscape analysis tool for topographic evaluation, drainage identification, watershed segmentation, and subcatchment parameterization: Overview. ARS-NAWQL 95-1. USDA-ARS National Agricultural Water Quality Laboratory. Durant, OK.

Gavigan, T. (2007.)Total maximum daily load for bedded sediment Blackwood Creek, Place County. Final Staff Report. South Lake Tahoe, CA: California Regional Water Quality Control Board. https://www.waterboards.ca.gov/lahontan/water_issues/programs/901 tmdl/blackwood/docs/blackwood_tmdl_final.pdf.

Giménez, R., Govers, G (2001) Interaction between bed roughness and flow hydraulics in eroding rills. *Water Resour. Res.* 37(3): 791–799.

Grant, G.E., Lewis, S.L., Swanson, F.J., Cissel, J.H., McDonnell, J.J. (2008) Effects of forest practices on peak flows and consequent channel response: A state-of-science report for Western Oregon and Washington. USDA, Pacific Northwest Research Station, General Technical Report PNW-GTR-760, Portland, OR.

Guerrant, D.G., Miller, W.W., Mahannah, C.N., Narayanan, R (1991) Site-Specific Erosivity Evaluation of a Sierra Nevada Forested Watershed Soil. *J. Env. Qual*. 20(2): 396–402.

Gupta, H.V., Kling, H., Yilmaz, K.K., Martinez, G.F. (2009) Decomposition of the mean squared error and NSE performance criteria: Implications for improving hydrological modelling, *J. Hydrol.* 377, 80–91.

Han, S.-K.; Han, H.-S. (2020) Productivity and cost of whole-tree and tree-length harvesting in fuel reduction thinning treatments using cable yarding systems. *For. Sci. Tech*. 16(1): 41–48.

Harrison, N.M., Stubblefield, A.P., Varner, J.M., Knapp, E.E. (2016) Finding balance between fire hazard reduction and erosion control in the Lake Tahoe Basin, California–Nevada. *For. Ecol. Manag*. 360: 40–51.

Hatch, L.K., Reuter, J.E., Goldman, C.R. (2001) Stream phosphorus transport in the Lake Tahoe basin, 1989–1996. *Environ. Monit. Assess*. 6 (9), 63–83.

Heron, T., Strawn, D.G., Dobre, M., Cade-Menun, B.J., Deval, C., Brooks, E.S., Piaskowski, J., Gasch, C., Crump, A. (2021) Soil phosphorus speciation and availability in meadows and forests in alpine lake watersheds with different parent material. *Front. For. Glob. Change*. 3:604200. doi:10.3389/ffgc.2020.604200.

Higuera, P.E., Abatzoglou, J.T. (2021) Record-setting climate enabled the extraordinary 2020 fire season in the western United States. *Glob. Chang. Biol*. 27, 1–2. doi:10.1111/gcb.15388.

Hyne, J.N., Chelminxki, P., Court, J.E., Gorsline, D.S., Goldman, C.R. (1972) Quaternary history of Lake Tahoe, California-Nevada. GSA Bulletin 83(5): 1435–1448.

Kattelmann, R. (1997) Flooding from rain-on-snow events in the Sierra Nevada. in: Leavesley , G.H., Lins, H.F., Nobilis, F., Randolph S.P., Schneider, V.R., Van de Ven, F.H.M. (Eds.), Destructive Water: Water-Caused Natural Disasters, Their Abatement and Control. IAHS Publication 239, Wallingford, Oxfordshire, UK. pp. 59–65.

Kaye, J.P., Hart, S.C., Fulé, P.Z., Covington, W.W., Moore, M.M., Kaye, M.W. (2005) Initial carbon, nitrogen, and phosphorus fluxes following ponderosa pine restoration treatments. *Ecol. Appl*. 15, 1581–1593. doi:10.1890/04-0868.

Kolden, C.A. (2019) We're not doing enough prescribed fire in the western United States to mitigate wildfire risk. *Fire* 2, 1–10. doi:10.3390/fire2020030.

Lake Tahoe Basin Report. 2014. Lake Tahoe Basin Multi-jurisdictional fuel reduction and wildfire prevention strategy. Online at: https://www.fs.usda.gov/Internet/FSE_DOCUMENTS/stelprd3812893.pdf

Lane, P.N.J., Sheridan, G.J., Noske, P.J., Sherwin, C.B. (2008) Phosphorus and nitrogen exports from SE Australian forests following wildfire. *J. Hydrol*. 361, 186–198. doi:10.1016/j.jhydrol.2008.07.041.

Lew, R., 2021. wepppy-win-bootstrap. https://github.com/rogerlew/wepppy-win-bootstrap. doi:10.5281/zenodo.4902236.

Lew, R., Dobre, M., Srivastava, A., Brooks, E.S., Elliot, W.J., Robichaud, P.R., Flanagan, D.C. (2021) WEPPcloud: An online watershed-scale hydrologic modeling tool. Part I. Model description. *J. Hydrol.* (*accepted*).

Long, J.W. (2009) Introduction to the effects of fuels management in the Tahoe basin. Effects of fuels management in the Lake Tahoe basin: a scientific literature review Final Report. Albany, CA: USDA Forest Service, Pacific Southwest Research Station. 10–41 pp.

Low, K.E., Collins, B.M., Bernal, A., Sanders, J.E., Pastor, D., Manley, P., White, A.M., Stephens, S.L. (2021) Longer-term impacts of fuel reduction treatments on forest structure, fuels, and drought resistance in the Lake Tahoe Basin. *For. Ecol. Manag.* 479:118609.

Mariotti, B., Hoshika, Y., Cambi, M., Marra, E., Feng, Z., Paoletti, E., Marchi, E. (2020) Vehicle-induced compaction of forest soil affects plant morphological and physiological attributes: A meta-analysis. *For. Ecol. Manag*. 462: 118004.

Marks, D., Link, T., Winstral, A., Garen, D. (2001) Simulating snowmelt processes during rain-on-snow over a semi-arid mountain basin. *Ann. Glaciol*. 32, 195–202.

Martin, C.W., Harr, R.D. (1989) Logging of mature Douglas-fir in western Oregon has little effect on nutrient output budgets. *Can. J. For. Res*. 19, 35–43. doi:10.1139/x89-005.

Mayer, P.M., Reynolds, S.K., Canfield, T.J., and McCutchen, M.D. (2005) Riparian buffer width, vegetative cover, and nitro-gen removal effectiveness: a review of current science and regulations. United States Environmental Protection Agency EPA/600/R-05/118.

McCabe, G.J., Clark, M.P., Hay, L.E. (2007) Rain-on-snow events in the western United States. *Bull. Am. Meteorol. Soc*. 88, 319–328. doi:10.1175/BAMS-88-3-319.

Murphy, J.D., Johnson, D.W., Miller, W.W., Walker, R.F., Carroll, E.F., Blank, R.R. (2006) Wildfire effects on soil nutrients and leaching in a Tahoe basin watershed. *J. Environ. Qual.* 35, 479–489. doi:10.2134/jeq2005.0144.

Nash, J., Sutcliffe, J.V. (1970) River flow forecasting through conceptual models part I—A discussion of principles. *J. Hydrol*., 10, 282–290.

Naslas, G.D., Miller, W.W., Gifford, G.F., Fernandez, G.C.J. (1994) Effects of soil type, plot condition, and slope on runoff and interrill erosion of two soils in the Lake Tahoe Basin. *J. Am. Water Res. Ass*. 30(2): 319–328.

Nearing, M.A., Deer-Ascough, L., Laflen, J.M. (1990) Sensitivity analysis of the WEPP hillslope profile erosion model. *Trans. ASAE* 33(3), 839–849.

Nicks, A.D., L.J. Lane, Gander, G.A. (1995) Chapter 2. Weather generator. in: Water Erosion Prediction Project: Hillslope Profile and Watershed Model Documentation, NSERL Report No. 10, (Eds.) Flanagan D.C. and Nearing, M.A. USDA Agricultural Research Service (ARS) National Soil Erosion Research Laboratory, West Lafayette, IN.

Nolan, K.M., Hill, B.R. (1991) Suspended-sediment budgets for four drainage basins tributary to Lake Tahoe, California and Nevada, 1984-87. USGS Water-Resources Investig. Rep. 91-4054. p 45.

Norman, S., Loupe, T., Keely, J. (2008) Heavenly Creek SEZ Demonstration Project 2007 Soil Monitoring Report. South Lake Tahoe, CA: USDA Forest Service Lake Tahoe Basin Management Unit. 58 p. https://www.fs.usda.gov/Internet/FSE_DOCUMENTS/fsm9_045987.pdf

Norman, S., Oehrli, C., Tolley, T., Brill, N. (2014) Blackwood Creek Reach 6 Restoration (Phase IIIA) Effectiveness Monitoring Results, UDSA Forest Service LTMU.

North, M., Brough, A., Long, J., Collins, B., Bowden, P., Yasuda, D., Miller, J., Sugihara, N. (2015) Constraints on mechanized treatment significantly limit mechanical fuels reduction extent in the Sierra Nevada. J. For. 113(1): 40–48.

Ottmar, R., Sandberg, D., Riccardi, C., Prichard S. (2007) An overview of the fuel characteristic classification system: Quantifying, classifying, and creating fuelbeds for resource planning, *Can. J. For. Res*., 37(12), 2383–2393.

Pell, C., Gross, S. (2016) Heavenly Creek SEZ Demonstration Project 2016 Vegetation Monitoring Report. South Lake Tahoe, CA: USDA Forest Service Lake Tahoe Basin Management Unit. 44 p. https://www.fs.usda.gov/Internet/FSE_DOCUMENTS/fseprd586255.pdf

Pietraszek, J.H. (2006) Controls on post-fire erosion at the hillslope scale, Colorado Front Range. MSc thesis, Colorado State University, Fort Collins.

Prats, S., Malvar, M., Coelho, C., Wagenbrenner, J. (2019) Hydrologic and erosion responses to compaction and added surface cover in post-fire logged areas: Isolating splash, interrill and rill erosion. J. *Hydrol*. 575: 408–419.

Runkel, R., Crawford, C., Cohn, T.A. (2004) Load Estimator (LOADEST): A FORTRAN Program for estimating constituent loads in streams and rivers: USGS Techniques and Methods, 4-A5. p. 75. http://pubs.usgs.gov/ tm/2005/tm4A5/.

Sánchez-Murillo, R., Brooks, E.S., Elliot, W.J., Gazel, E., Boll, J. (2014) Baseflow recession analysis in the inland Pacific Northwest of the United States. Hydrogeol. J. 23, 287–303.

Santín, C., Otero, X.L., Doerr, S.H., Chafer, C.J. (2018) Impact of a moderate/high-severity prescribed eucalypt forest fire on soil phosphorous stocks and partitioning. *Sci. Total Environ*. 621: 1103–1114.

Safford, H.D., Schmidt, D.A., Carlson, C.H. (2009) Effects of fuel treatments on fire severity in an area of wildland–urban interface, Angora Fire, Lake Tahoe Basin, California. Forest Ecology and Management. 258(5): 773–787.

Scheller, R.M., Domingo, J.B., Sturtevant, B.R., Williams, J.S., Rudy, A., Gustafson, E.J., Mladenoff, D.J. (2007) Design, development, and application of LANDIS-II, a spatial landscape simulation model with flexible temporal and spatial resolution. *Ecol. Model.* 201(3–4):409–419.

Schwilk, DW, Keeley, J.E., Knapp, E.E., McIver, J., Bailey, J.D., Fettig, C.J., Fiedler, C.E., Harrod, RJ, Moghaddas, J.J., Outcalt, K.W., Skinner, C.N., Stephens, S.L., Waldrop, T.A., Yaussy, D.A., Youngblood, A. (2009) The national fire and fire surrogate study: effects of fuel reduction methods on forest vegetation structure and fuels. *Ecol Appl* 19:285–304

Sidle, R.C. Ziegler, A.D. Negishi, J.N. Nik, A.R. Siew, R. Turkelboom, F. (2006) Erosion processes in steep terrain—Truths, myths, and uncertainties related to forest management in Southeast Asia. *Catchment Processes in Southeast Asia*. 224(1): 199–225.

Simon, A., Langendoen, E., Bingner, R., Wells, R., Heins, A., Jokay, N., Jaramillo, I. (2004) Lake Tahoe Basin framework implementation study: sediment loadings and channel erosion. USDA-ARS National Sedimentation Laboratory Research Report. No. 39. pp. 377.

Simon, A., Pollen-Bankhead, N., Mahacek, V., Langendoen, E. (2009) Quantifying reductions of mass-failure frequency and sediment loadings from streambanks using toe protection and other means: Lake Tahoe, United States. *J. Am. Water Resour*. As. 45(1): 170–186. doi: 10.1111/j.1752-1688.2008.00268.x.

Smith, H.G., Sheridan, G.J., Lane, P.N.J., Nyman, P., Haydon, S. (2011) Wildfire effects on water quality in forest catchments: A review with implications for water supply. *J. Hydrol*. 396, 170–192. doi:10.1016/j.jhydrol.2010.10.043.

Spigel, K.M., Robichaud, P.R. (2007) First-year post-fire erosion rates in Bitterroot National Forest, Montana. *Hydrol. Process*. 21, 988–1005.

Srivastava, A., Dobre, M., Wu, J.Q., Elliot, W.J., Bruner, E.A., Dun, S., Brooks, E.S., Miller, I.S. (2013) Modifying WEPP to improve streamflow simulation in a Pacific Northwest watershed. *Trans. ASABE* 56(2):603–611.

Srivastava, A., Wu, J.Q., Elliot, W.J., Brooks, E.S., Flanagan, D.C. (2017) Modeling streamflow in a snow-dominated forest watershed using the water erosion prediction project (WEPP) model. *Trans. ASABE* 60, 1171–1187. doi:10.13031/trans.12035.

Srivastava, A., Wu, J.Q., Elliot, W.J., Brooks, E.S. and Flanagan, D.C. (2018) A simulation study to estimate effects of wildfire and forest management on hydrology and sediment in a forested watershed, Northwestern U.S. *Trans. ASABE* 61(5), 1579–1601. https://doi.org/10.13031/trans.12326.

Srivastava, A., Flanagan, D.C., Frankenberger, J.R., Engel, B.A. (2019) Updated climate database and impacts on WEPP model predictions. *J. Soil Water Conserv*. 74, 334–349. doi:10.2489/jswc.74.4.334.

Srivastava A., Brooks E.S., Dobre M., Elliot W.J., Link T.E. (2020) Modeling forest management effects on water and sediment yield from nested, paired watersheds in the interior Pacific Northwest, USA using WEPP. *Sci. Total Environ*. 701:134877.

Tetra Tech Inc. (2007) Watershed hydrologic modeling and sediment and nutrient loading estimation for the Lake Tahoe total maximum daily load. Final Modeling Report. Lahontan Reg. Water Quality Control Board, South Lake Tahoe, CA.

Thornton, M.M., Thornton, P.E., Wei, Y., Mayer, B.W., Cook, R.B., Vose, R.S. (2016) Daymet: Monthly Climate Summaries on a 1-km Grid for North America, Version 3. ORNL DAAC, Oak Ridge, Tennessee, USA. http://dx.doi.org/10.3334/ORNLDAAC/1345.

Verburg, P.S.J., Miller, W.W., Busse, M.D., Rice, E., Grismer, M.E. (2009) Soil and water quality response to fuels management in the Lake Tahoe Basin. Effects of fuels management in the Lake Tahoe basin: a scientific literature review Final Report. Albany, CA: USDA Forest Service, Pacific Southwest Research Station. 116–183 pp.

Wang, L., Wu, J.Q., Elliot, W.J., Fiedler, F.R., Lapin, S. (2014) Linear diffusion wave channel routing using a discrete Hayami convolution method, *J. Hydrol*., 509, 282–294.

Westerling, A.L., Hidalgo, H.G., Cayan, D.R., Swetnam, T.W. (2006) Warming and earlier spring increase western US forest wildfire activity. *Science* 313, 940–943.

Williams, A.P., Abatzoglou, J.T., Gershunov, A., Guzman-Morales, J., Bishop, D.A., Balch, J.K., Lettenmaier, D.P. (2019) Observed impacts of anthropogenic climate change on wildfire in California. *Earth's Future*, 7, 892−910.

Yapo, P., Gupta, H.V., Sorooshian, S. (1996) Calibration of conceptual rainfall-runoff models: sensitivity to calibration data, *J. Hydrol*., 181, 23–48.

Yue X., Mickley, L.J., Logan, J.A. (2014) Projection of wildfire activity in southern California in the mid-twenty-first century. *Clim. Dyn*. 43:1973–1991.

Zambrano-Bigiarini, M. (2020) hydroGOF: Goodness-of-fit functions for comparison of simulated and observed hydrological time series. doi: 10.5281/zenodo.839854, R package version 0.4–0, https://github.com/hzambran/hydroGOF.

Zamora-Cristales, R., Adams, P.W., Sessions, J. (2014) Ground-Based Thinning on Steep Slopes in Western Oregon: Soil Exposure and Strength Effects. *For. Sci*. 60(5): 1014–1020.

Zaslavsky, D., Rogowski, A.S. (1969) Hydrologic and morphologic implications of anisotropy and infiltration in soil profile development. *Soil Sci. Soc. Am. J.* 33(4), 594–599. https://doi.org/10.2136/sssaj1969.03615995003300040031x

APPENDIX

Interpolated values of baseflow, deep seepage, channel critical shear, and phosphorus.

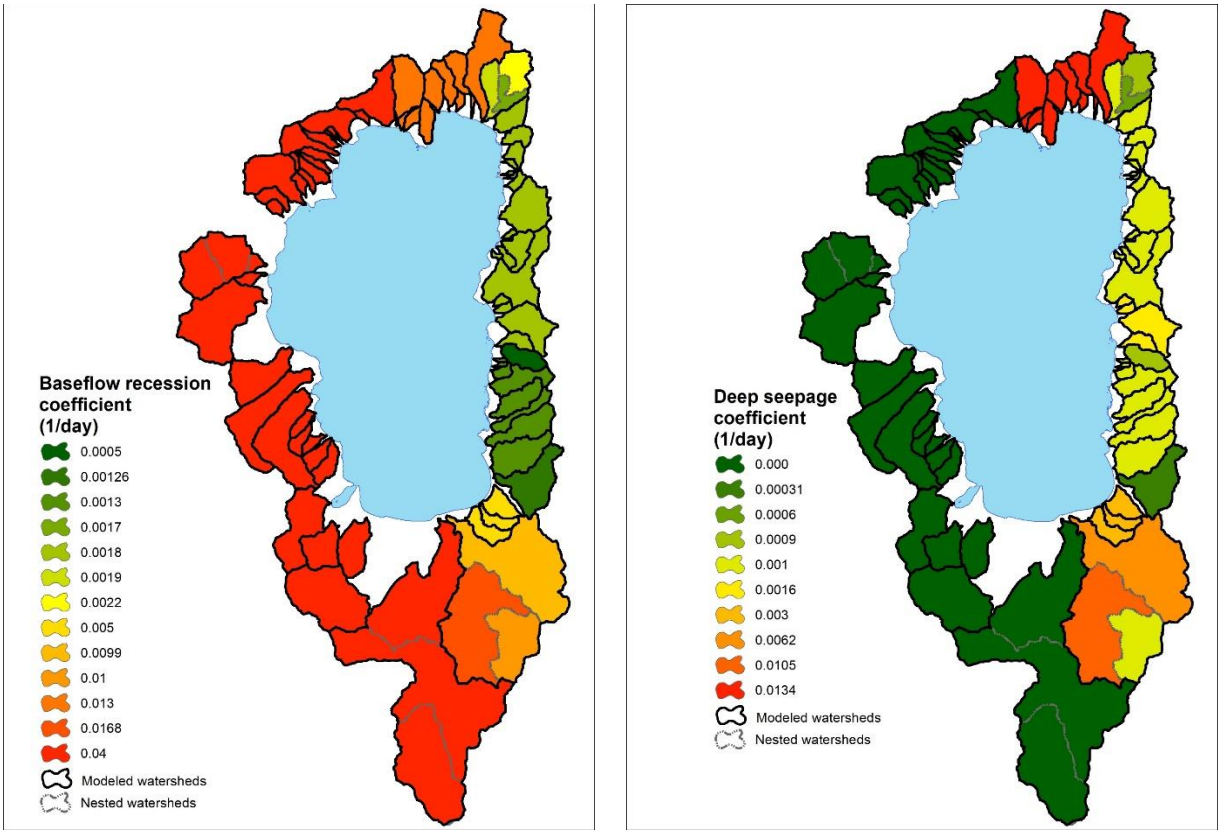

Figure A1. Interpolated estimated values of baseflow and deep seepage recession coefficients for Lake Tahoe basin watersheds in California/ Nevada.

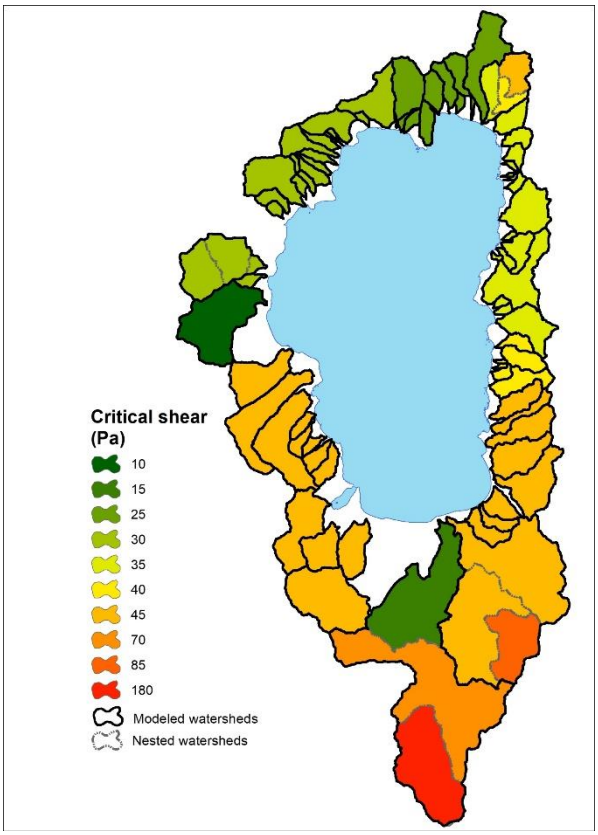

Figure A2. Interpolated channel critical shear for Lake Tahoe basin watersheds in California/ Nevada.

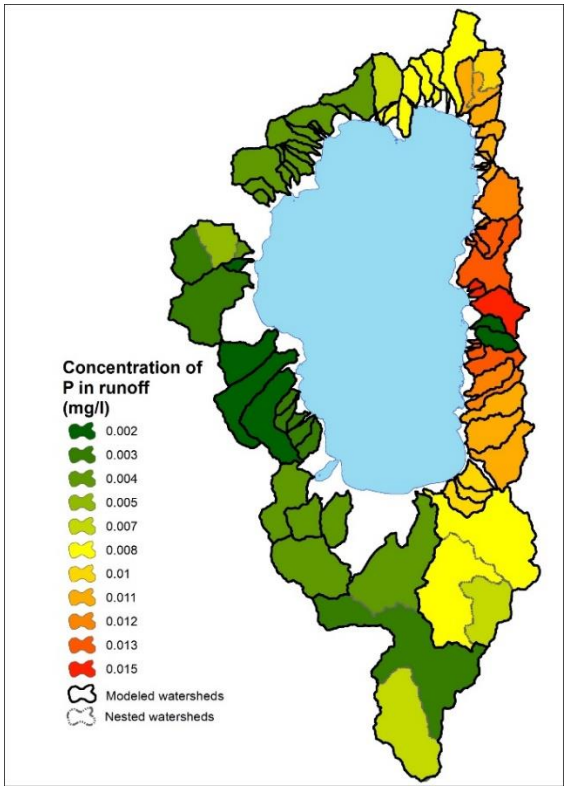
Concentration of
P in runoff
(mg/l)
0.002
0.003
0.004
0.005
0.007
0.008
0.01
0.011
0.012
0.013
0.015
Modeled watersheds
Nested watersheds

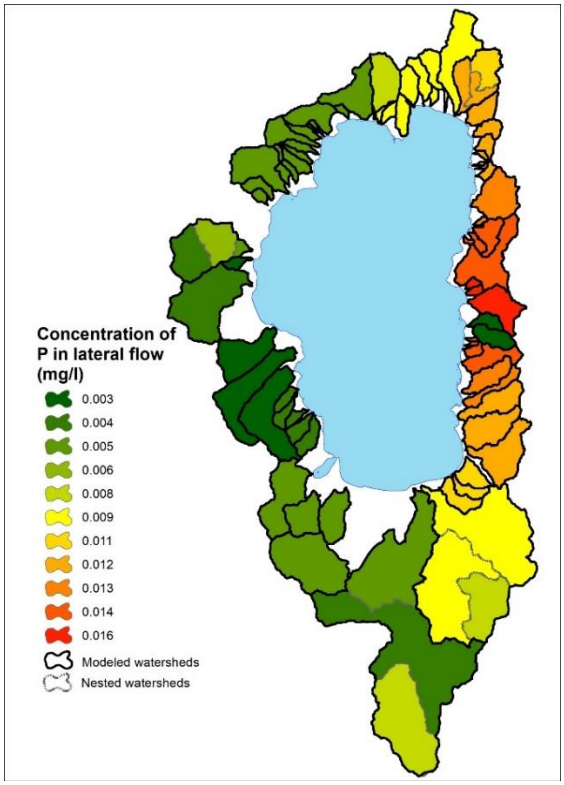
Concentration of
P in lateral flow
(mg/l)
0.003
0.004
0.005
0.006
0.008
0.009
0.011
0.012
0.013
0.014
0.016
Modeled watersheds
Nested watersheds

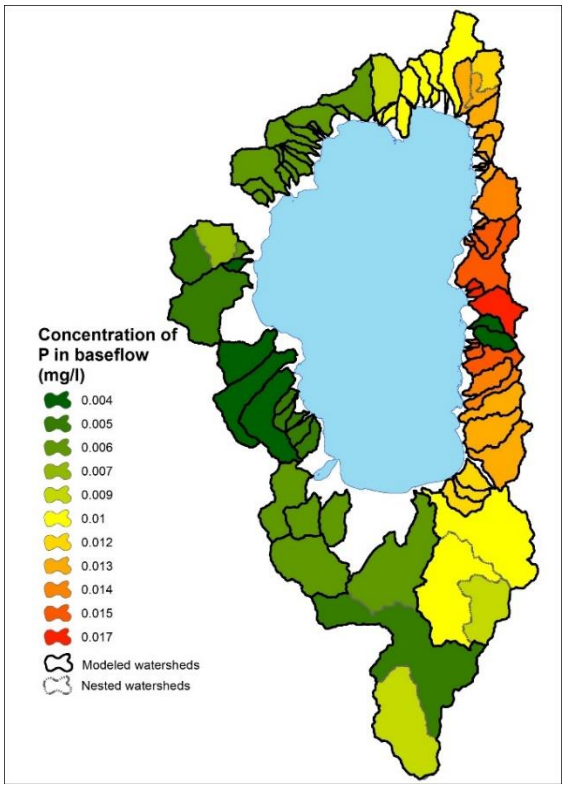
Concentration of
P in baseflow
(mg/l)
0.004
0.005
0.006
0.007
0.009
0.01
0.012
0.013
0.014
0.015
0.017
Modeled watersheds
Nested watersheds

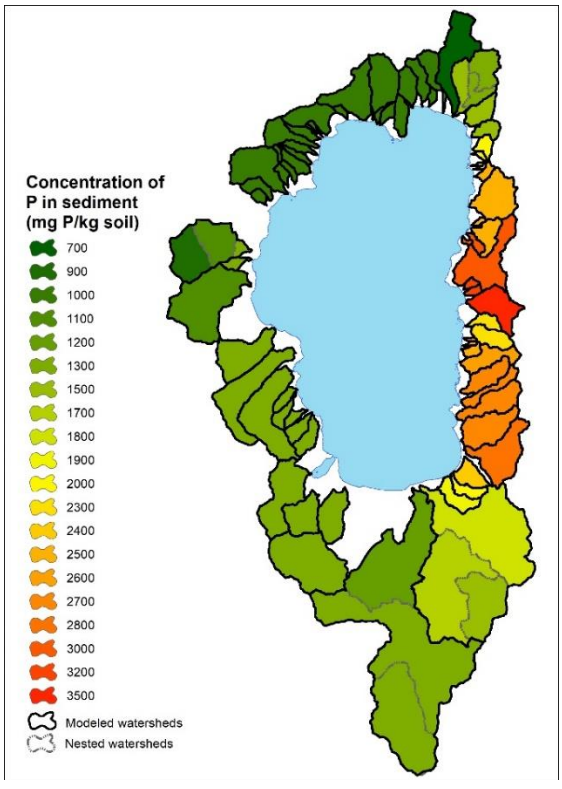
Concentration of
P in sediment
(mg P/kg soil)
700
900
1000
1100
1200
1300
1500
1700
1800
1900
2000
2300
2400
2500
2600
2700
2800
3000
3200
3500
Modeled watersheds
Nested watersheds

Figure A3. Interpolated phosphorus concentrations in runoff, lateral flow, baseflow and sediment from Lake Tahoe basin watersheds in California/Nevada.

Table A1. Watershed information and web links to model runs.

No.	Name	USGS station	USGS Name/Watershed Name Location
			California
1	WC8	10336676	WARD C AT HWY 89 NR TAHOE PINES https://wepp.cloud/weppcloud/runs/lt_202012_63_Ward_Creek_CurCond/cfg/
2	WC7A	10336675	WARD C A STANFORD ROCK TRAIL XING NR TAHOE CITY https://wepp.cloud/weppcloud/runs/lt_202012_63_Ward_Creek_WC3A_CurCond/cfg/
3	WC3A	10336674	WARD C BL CONFLUENCE NR TAHOE CITY https://wepp.cloud/weppcloud/runs/lt_202012_63_Ward_Creek_WC7A_CurCond/cfg/
4	BC1	10336660	BLACKWOOD C NR TAHOE CITY https://wepp.cloud/weppcloud/runs/lt_202012_62_Blackwood_Creek_CurCond/cfg/
5	GC1	10336645	GENERAL C NR MEEKS BAY https://wepp.cloud/weppcloud/runs/lt_202012_56_General_Creek_CurCond/cfg/
6	UTR1	10336610	UPPER TRUCKEE RV AT SOUTH LAKE TAHOE https://wepp.cloud/weppcloud/runs/lt_202012_44_Upper_Truckee_River_Big_Meadow_Creek_CurCond/cfg/
7	UTR3	103366092	UPPER TRUCKEE RV AT HWY 50 ABV MEYERS https://wepp.cloud/weppcloud/runs/lt_202012_44_Upper_Truckee_River_UT3_CurCond/cfg/
8	UTR5	10336580	UPPER TRUCKEE RV AT S UPPER TRUCKEE RD NR MEYERS https://wepp.cloud/weppcloud/runs/lt_202012_44_Upper_Truckee_River_UT5_CurCond/cfg/
9	TC4	10336780	TROUT CK NR TAHOE VALLEY https://wepp.cloud/weppcloud/runs/lt_202012_43_Trout_Creek_CurCond/cfg/
10	TC2	10336775	TROUT CK AT PIONEER TRAIL NR SOUTH LAKE TAHOE https://wepp.cloud/weppcloud/runs/lt_202012_43_Trout_Creek_TC2_CurCond/cfg/
11	TC3	10336770	TROUT CK AT USFS RD 12N01 NR MEYERS https://wepp.cloud/weppcloud/runs/lt_202012_43_Trout_Creek_TC3_CurCond/cfg/
			Nevada
12	LH1	10336740	LOGAN HOUSE CK NR GLENBROOK https://wepp.cloud/weppcloud/runs/lt_202012_31_Logan_House_Creek_CurCond/cfg/
13	GL1	10336730	GLENBROOK CK AT GLENBROOK https://wepp.cloud/weppcloud/runs/lt_202012_29_Glenbrook_Creek_CurCond/cfg/
14	IN1	10336700	INCLINE CK NR CRYSTAL BAY https://wepp.cloud/weppcloud/runs/lt_202012_19_Incline_Creek_CurCond/cfg/
15	IN2	103366995	INCLINE CK AT HWY 28 AT INCLINE VILLEGE https://wepp.cloud/weppcloud/runs/lt_202012_19_Incline_Creek_IN2_CurCond/cfg/
16	IN3	103366993	INCLINE CK ABV TYROL VILLAGE NR INCLINE VILLAGE https://wepp.cloud/weppcloud/runs/lt_202012_19_Incline_Creek_IN3_CurCond/cfg/
17	TH1	10336698	THIRD CK NR CRYSTAL BAY https://wepp.cloud/weppcloud/runs/lt_202012_18_Third_Creek_CurCond/cfg/